
Robust Imitation via Mirror Descent Inverse Reinforcement Learning

Dong-Sig Han, Hyunseo Kim, Hyundo Lee, Je-Hwan Ryu, Byoung-Tak Zhang

Artificial Intelligence Institute, Seoul National University

{dshan, hskim, hdlee, jhryu, btzhang}@bi.snu.ac.kr

Abstract

Recently, adversarial imitation learning has shown a scalable reward acquisition method for inverse reinforcement learning (IRL) problems. However, estimated reward signals often become uncertain and fail to train a reliable statistical model since the existing methods tend to solve hard optimization problems directly. Inspired by a first-order optimization method called mirror descent, this paper proposes to predict a sequence of reward functions, which are iterative solutions for a constrained convex problem. IRL solutions derived by mirror descent are tolerant to the uncertainty incurred by target density estimation since the amount of reward learning is regulated with respect to local geometric constraints. We prove that the proposed mirror descent update rule ensures robust minimization of a Bregman divergence in terms of a rigorous regret bound of $\mathcal{O}(1/T)$ for step sizes $\{\eta_t\}_{t=1}^T$. Our IRL method was applied on top of an adversarial framework, and it outperformed existing adversarial methods in an extensive suite of benchmarks.

1 Introduction

One crucial requirement of practical imitation learning methods is *robustness*, often described as learning expert behavior for a finite number of demonstrations, overcoming various realistic challenges [1]. In real-world problems such as motor control tasks, the demonstration size can be insufficient to create a precise model of an expert [2], and even in some cases, demonstrations can be noisy or suboptimal to solve the problem [3]. For such challenging scenarios, imitation learning algorithms inevitably struggle with unreliable statistical models; thus, the way of handling the uncertainty of estimated cost functions dramatically affects imitation performance. Therefore, a thorough analysis of addressing these issues is required to construct a robust algorithm.

Inverse reinforcement learning (IRL) is an algorithm for learning ground-truth rewards from expert demonstrations where the expert acts optimally with respect to an unknown reward function [4, 5]. Traditional IRL studies solve the imitation problem based on iterative algorithms [6, 7], alternating between the reward estimation process and a reinforcement learning (RL) [8] algorithm. In contrast, newer studies of adversarial imitation learning (AIL) [9, 10] rather suggest learning reward functions of a certain form “directly,” by using adversarial learning objectives [11] and nonlinear discriminative neural networks [10]. Compared to classical approaches, the AIL methods have shown great success on control benchmarks in terms of scalability for challenging control tasks [12].

Technically, it is well known that AIL formulates a divergence minimization problem with its discriminative signals, which incorporates fine-tuned estimations of the target densities [13]. Through the lens of differential geometries, the limitation of AIL naturally comes from the implication that minimizing the divergence does not guarantee unbiased progression due to constraints of the underlying space [14]. In order to ensure further stability, we argue that an IRL algorithm’s progress needs to be regulated, yielding gradual updates with respect to local geometries of policy distributions.

We claim that there are two issues leading to unconstrained policy updates: ① a statistical divergence often cannot be accurately obtained for challenging problems, and ② an immediate divergence between agent and expert densities does not guarantee unbiased learning directions. Our approach is connected to a collection of optimization processes called mirror descent (MD) [15]. For a sequence of parameters $\{w_t\}_{t=1}^T$ and a convex function Ω , an MD update for a cost function F_t is derived as

$$\nabla\Omega(w_{t+1}) = \nabla\Omega(w_t) - \eta_t \nabla F_t(w_t). \quad (1)$$

In the equation, the gradient $\nabla\Omega(\cdot)$ creates a transformation that links a parametric space to its dual space. Theoretically, MD is a first-order method for solving constrained problems, which enjoys rigorous regret bounds for various geometries [16, 17] including probability spaces. Thus, applying MD to the reward estimation process can be efficient in terms of the number of learning phases.

In this paper, we derive an MD update rule in IRL upon a postulate of nonstationary estimations of the expert density, resulting in convergent reward acquisition even for challenging problems. Compared to MD algorithms in optimization studies, our methodology draws a sequence of functions on an alternative space induced by a reward operator Ψ_Ω (Definition 1). To this end, we propose an AIL algorithm called mirror descent adversarial inverse reinforcement learning (MD-AIRL). Our empirical evidence showed that MD-AIRL outperforms the regularized adversarial IRL (RAIRL) [18] methods. For example, MD-AIRL showed higher performance in 30 distinct cases among 32 different configurations in challenging MuJoCo [19] benchmarks, and it also clearly showed higher tolerance to suboptimal data. All of these results are strongly aligned with our theoretical analyses.

Table 1: A technical overview. Traditional IRL methods lack scalability, and RAIRL does not guarantee convergence of its solution for realistic cases. MD-AIRL combines desirable properties.

Method	Reference	Scalability	Rewards	Bregman divergence	Iterative solutions	Convergence analyses
BC (1991)	[20]	✓	✗	✗	✗	✓
MM-IRL (2004)	[6]	✗	✓	✗	✓	✓
GAIL (2016)	[9]	✓	✓	✗	✗	✗
RAIRL (2021)	[18]	✓	✓	✓	✗	✗
MD-AIRL (ours)	-	✓	✓	✓	✓	✓

Our contributions. Our work is complementary to previous IRL studies; the theoretical and technical contributions are built upon a novel perspective of considering iterative RL and IRL algorithms as a combined optimization process with dual aspects. Comparing MD-AIRL and RAIRL, both are highly generalized algorithms in terms of a variety of choices of divergence functions. Tab. 1 shows that MD-AIRL brings beneficial results in realistic situations of limited time and data, since our approach is more aligned with earlier theoretical IRL studies providing formalized reward learning schemes and convergence guarantees. In summary, we list our main contributions below:

- Instead of a monolithic estimation process of a global solution in AIL, we derive a sequence of reward functions that provides iterative local objectives (Section 4).
- We formally prove that rewards derived by an MD update rule guarantee the robust performance of divergence minimization along with a rigorous regret bound (Section 5).
- We propose a novel adversarial algorithm that is motivated by mirror descent, which is tolerant of unreliable discriminative signals of the AIL framework (Sections 6 and 7).

2 Related Works

Mirror descent. We are interested in a family of statistical divergences called the Bregman divergence [21]. The divergence generalizes constrained optimization problems such as least squares [22, 23], and it also has been applied in various subfields of machine learning [24, 25]. In differential geometries, the Bregman divergence is a first-order approximation for a metric tensor and satisfies metric-like properties [14, 26]. MD is also closely related to optimization methods regarding non-Euclidean geometries with a discretization of steps such as natural gradients [27, 28]. In the primal space, training with the infinitesimal limit of MD steps corresponds to a Riemannian gradient flow [29, 30]. In the RL domain, MD has been recently studied for policy optimization [31–33]. In this paper, we focus on learning with suboptimal representations of policy, and our distinct goal is to draw a robust reward learning scheme based on MD for the IRL problem.

Imitation learning. As a statistical model for the information geometry [34], energy-based policies (i.e., Boltzmann distributions) appeared in early IRL studies, such as Bayesian IRL, natural gradient

IRL, and maximum likelihood IRL [35–37] for modeling expert distribution to parameterized functions. Notably, MaxEnt IRL [7, 38] is one of the representative classical IRL algorithms based on an information-theoretic perspective toward IRL solutions. Also, discriminators of AIL are trained by logistic regression; thus, the logit score of the discriminator defines an energy function that approximates the truth data density for the expert distribution [39]. Other statistical entropies have also been applied to AIL, such as the Tsallis entropy [40]. On the one hand, our approach is closely related to RAIRL [18], which defined its AIL objective using the Bregman divergence. On the other hand, this work further employs the Bregman divergence to derive iterative MD updates for reward functions, resulting in theoretically pleasing properties while retaining the scalability of AIL.

Learning theory. There have been considerable achievements in dealing with temporal costs $\{F_t\}_{t=1}^\infty$, often referred to as *online learning* [41]. The most ordinary approach is stochastic gradient descent (SGD): $w_{t+1} = w_t - \eta_t \nabla F_t(w_t)$. In particular, SGD is a desirable algorithm when the parameter w_t resides in the Euclidean space since it ensures unbiased minimization of the expected cost. Apparently, policies appear in geometries of probabilities; thus, an incurred gradient may not be the direction of the steepest descent due to geometric constraints [27, 34]. An online form of MD in Eq. (1) is analogous to SGD for non-Euclidean spaces, where each local metric is specified by a Bregman divergence [30]. Our theoretical findings and proofs follow the results of online mirror descent (OMD) that appeared in previous literature for general aspects [15, 16, 42, 28, 17, 30]. Our analyses extend existing theoretical results to IRL; at the same time, they are also highly general to cover various online imitation learning problems which require making decisions sequentially.

3 Background

For sets X and Y , let Y^X be a set of functions from X to Y and Δ_X (Δ_X^Y) be a set of (conditional) probabilities over X (conditioned on Y). We consider an MDP defined as a tuple $(\mathcal{S}, \mathcal{A}, P, r, \gamma)$ with the state space \mathcal{S} , the action space \mathcal{A} , the Markovian transition kernel $P \in \Delta_{\mathcal{S}}^{\mathcal{S} \times \mathcal{A}}$, the reward function $r \in \mathbb{R}^{\mathcal{S} \times \mathcal{A}}$ and the discount factor $\gamma \in [0, 1)$. Let a function $\Omega: \Delta_{\mathcal{A}} \rightarrow \mathbb{R}$ be strongly convex. Using Ω , the Bregman divergence is defined as

$$D_\Omega(\pi^s \parallel \hat{\pi}^s) := \Omega(\pi^s) - \Omega(\hat{\pi}^s) - \langle \nabla \Omega(\hat{\pi}^s), \pi^s - \hat{\pi}^s \rangle_{\mathcal{A}},$$

where π^s and $\hat{\pi}^s$ denote arbitrary policies for a given state s . For a representative divergence, one can consider the popular Kullback-Leibler (KL) divergence. The KL divergence is a Bregman divergence when Ω is specified as the negative Shannon entropy: $\Omega(\pi^s) = \sum_a \pi^s(a) \ln \pi^s(a)$.

Regularization of the policy distribution with respect to convex Ω brings distinct properties to the learning agent [43, 44]. The objective of regularized RL is to find $\pi \in \Pi$ that maximizes the expected value of discounted cumulative returns along with a causal convex regularizer Ω , i.e.,

$$J_\Omega(\pi, r) := \mathbb{E}_\pi \left[\sum_{i=0}^\infty \gamma^i \left\{ r(s_i, a_i) - \Omega(\pi(\cdot | s_i)) \right\} \right], \quad (2)$$

where the subscript π on the expectation indicates that each action is sampled by $\pi(\cdot | s_i)$ for the given MDP. In this setup, a regularized RL algorithm finds a unique solution in a subset of the conditional probability space denoted as $\Pi := [\Pi^s]_{s \in \mathcal{S}} \subset \Delta_{\mathcal{A}}^{\mathcal{S}}$ constrained by the parameterization of a policy.

The objective of IRL is to find a function r_E that rationalizes the behavior of an expert policy π_E . For an inner product $\langle \cdot, \cdot \rangle_{\mathcal{A}}$, consider Ω^* , the Legendre-Fenchel transform (convex conjugate) of Ω :

$$\forall q^s \in \mathbb{R}^{\mathcal{A}}, \quad \Omega^*(q^s) = \max_{\pi^s \in \Delta_{\mathcal{A}}} \langle \pi^s, q^s \rangle_{\mathcal{A}} - \Omega(\pi^s), \quad (3)$$

where q^s and π^s denote the shorthand notation of $q(s, \cdot)$ and $\pi(\cdot | s)$. Differentiating both sides with respect to q^s , the gradient of conjugate $\nabla \Omega^*$ maps q^s to a policy distribution. One fundamental property in *regularized IRL* [43] is that π_E is the maximizing argument of Ω^* for q_E , where q_E is the regularized state-action value function $q_E(s, a) = \mathbb{E}_{\pi_E} [\sum_{i=0}^\infty \gamma^i \{r_E(s, a) - \Omega(\pi_E^s)\}] |_{s_0=s, a_0=a}$. Note that the problem is ill-posed, and every \hat{r}_E that makes its value function \hat{q}_E satisfy $\pi_E^s = \nabla \Omega^*(\hat{q}_E^s) \forall s \in \mathcal{S}$ is a valid solution. Addressing this issue, Jeon et al. [18] proposed a reward operator $\Psi_\Omega: \Delta_{\mathcal{A}}^{\mathcal{S}} \rightarrow \mathbb{R}^{\mathcal{S} \times \mathcal{A}}$, providing a unique IRL solution by $\Psi_\Omega(\pi_E)$.

Definition 1 (Regularized reward operators). Define the regularized reward operator Ψ_Ω as $\psi_\pi(s, a) := \Omega'(s, a; \pi) - \langle \pi^s, \nabla \Omega(\pi^s) \rangle_{\mathcal{A}} + \Omega(\pi^s)$, for $\Omega'(s, \cdot; \pi) := \nabla \Omega(\pi^s) = [\nabla_p \Omega(p)]_{p=\pi(\cdot | s)}$.

The reward function $\psi_E := \Psi_\Omega(\pi_E)$ replaces its state-action value function, since the sum of composite Bregman divergences derived from Eq. (2) allows reward learning in a greedy manner [18].

4 RL-IRL as a Proximal Method

Associated reward functions. We consider the RL-IRL processes as a sequential algorithm with local constraints and define sequences $\{\pi_t\}_{t=1}^\infty$ and $\{\psi_t\}_{t=1}^\infty$ that denote policies and associated reward functions, respectively. The associated reward functions are in a space $\Psi_\Omega(\Pi)$, which is an alternative space of the dual space, defined by the regularized reward operator Ψ_Ω . Formally, we provide Lemma 1, which shows a bijective relation between the operators $\nabla\Omega^*$ and Ψ_Ω in the set Π . The proof is in Appendix A.

Lemma 1 (Natural isomorphism). *Let $\psi \in \Psi_\Omega(\Pi)$ for $\Psi_\Omega(X) := \{\psi \mid \psi(s, a) = \psi_\pi(s, a), \forall s \in \mathcal{S}, a \in \mathcal{A}, \pi \in X\}$. Then, $\nabla\Omega^*(\psi)$ is unique and for every $\pi = \nabla\Omega^*(\psi)$, $\pi \in \Pi$.*

Fig. 1 illustrates that there is a unique ψ_t for π_t in every time step. Note that $\Psi_\Omega(\pi_t)$ is different from $\nabla\Omega(\pi_t)$; it is shifted by a vector $\mathbf{1}c$ with a constant $c = \Omega(\pi_t^s) - \langle \pi_t^s, \nabla\Omega(\pi_t^s) \rangle_{\mathcal{A}}$. Since the underlying space is a probability simplex, the operator $\nabla\Omega^*$ reconstructs the original point for both Ψ_Ω and $\nabla\Omega$, as the distributivity [43] $\Omega^*(y + \mathbf{1}c) = \Omega^*(y) + c$ holds (so $\nabla\Omega^*(y + \mathbf{1}c) = \nabla\Omega^*(y)$). An alternative interpretation is of considering a projection (gray dashed line in Fig. 1). Suppose that a policy π_t is updated to $\tilde{\pi}_{t+1} \in \mathbb{R}^{\mathcal{S} \times \mathcal{A}}$. The Bregman projection operator \mathcal{P}_Ω is applied that locates the subsequent update π_{t+1} to the “feasible” region, i.e., $\mathcal{P}_\Omega(\tilde{\pi}_{t+1}) := \operatorname{argmin}_{\pi \in \Pi} [D_\Omega(\pi^s \parallel \tilde{\pi}_{t+1}^s)]_{s \in \mathcal{S}}$.

Consequently, one can consider an updated reward function ψ_{t+1} as a projected target of MD associated with an alternative parameterization of Π . For instance, the parameters of ψ_t can construct a softmax policy for a discrete space, or a Gaussian policy for a continuous space. Using the reward function ψ_{t+1} , an arbitrary regularized RL process maximizing Eq. (2) at the t -th step [18]

$$J_\Omega(\pi, \psi_{t+1}) = -\mathbb{E}_\pi \left[\sum_{i=0}^{\infty} \gamma^i D_\Omega \left(\pi(\cdot | s_i) \parallel \pi_{t+1}(\cdot | s_i) \right) \right] \quad (4)$$

becomes finding the next iteration $\pi_{t+1} = \nabla\Omega^*(\psi_{t+1})$ by maximizing the expected cumulative return. The equation shows that a regularized RL algorithm with the regularizer Ω forms a cumulative sum of Bregman divergences; thus, the policy π_{t+1} is uniquely achieved by the property of divergence.

Online imitation learning. Our setup starts from the apparent yet vital premise that an imitation learning algorithm does not retain the global target π_E during training. That is, it is fundamentally uncertain to model global objectives (such as $J_\Omega(\pi, \psi_E)$), which are not attainable for both RL and IRL. Instead, we hypothesize on the existence of a random process $\{\bar{\pi}_{E,t}\}_{t=1}^\infty$ where each estimation $\bar{\pi}_{E,t}$ resides in a closed, convex neighborhood of π_E , generated by an arbitrary estimation algorithm. Substituting ψ_E to $\psi_{\bar{\pi}_{E,t}} = \Psi_\Omega(\bar{\pi}_{E,t})$, the nonstationary objective $J_\Omega(\pi, \psi_{\bar{\pi}_{E,t}})$ forms a temporal cost:

$$F_t(\pi) = \mathbb{E}_\pi \left[\sum_{i=0}^{\infty} \gamma^i D_\Omega \left(\pi(\cdot | s_i) \parallel \bar{\pi}_{E,t}(\cdot | s_i) \right) \right]. \quad (5)$$

For the sake of better understanding, we considered an actual experiment depicted in Fig. 2. Suppose that the policies of the learning agent and the expert follow multivariate Gaussian distributions at

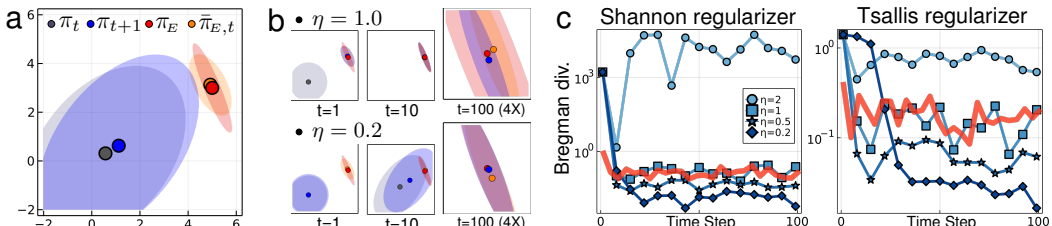


Figure 2: (a) A policy π_t learns from MD updates for temporal costs $D_\Omega(\cdot \parallel \bar{\pi}_{E,t})$. (b) The updates of π_t vary by η , and the distance between π_t and π_E can be closer than the distance between $\bar{\pi}_{E,t}$ and π_E when t is sufficiently large and the η is effectively low. (c) Two plots show $D_\Omega(\pi_t, \parallel \pi_E)$ associated with entropic regularizers for four different η (10 trials), with the red baselines $D_\Omega(\bar{\pi}_{E,t} \parallel \pi_E)$.

Figure 1: A schematic illustration. MD is locally constrained by a divergence (gray area), i.e., $D_\Omega(\cdot \parallel \pi_t)$. An MD update is performed for the reward function ψ_t in an associated reward space of defined by Ψ_Ω , and π_{t+1} is achieved in the desired space of Π by applying $\nabla\Omega^*$ for the function ψ_{t+1} . The gray dashed lines provide another interpretation of MD with $\tilde{\pi}_{t+1}$ and the projection operator \mathcal{P}_Ω .

$\mathcal{N}([0, 0]^T, \mathbf{I})$ and $\mathcal{N}([5, 3]^T, \Sigma_E)$ with $|\Sigma_E| < 1$. Let a (suboptimal) reference policy $\bar{\pi}_{E,t}$ be independently fitted with a maximum likelihood estimator with a relatively high learning rate, starting from $\bar{\pi}_{E,1} = \pi_1$. The policy π_t was trained by a cost function $D_\Omega(\cdot \parallel \bar{\pi}_{E,t})$ using the MD update rule in Eq. (1). In Fig. 2, we first observed that choosing a high step size constant η accelerated the training speed mainly in the early phase. The results also showed that the performance of MD ($D_\Omega(\pi_t \parallel \pi_E)$) outperformed that of referenced maximum likelihood estimation ($D_\Omega(\bar{\pi}_{E,t} \parallel \pi_E)$) by choosing an effectively low step size. This empirical evidence suggests that there are clear advantages in formalization of the training steps and scheduling the step sizes, especially for unreliable statistical model $\bar{\pi}_{E,t}$.

MD update rules. As a result of these findings, we formulate subsequent MD steps with a regularized reward function. Let w_t be a parameter on a set \mathcal{W} and $F_t : \mathcal{W} \rightarrow \mathbb{R}$ be a convex cost function from a class of functions \mathcal{F} at the t -th step. Replacing the L2 proximity term of proximal gradient descent with a Bregman divergence, the proximal form of the MD update for Eq. (1) is written as [45]

$$\underset{w \in \mathcal{W}}{\text{minimize}} \langle \nabla F_t(w_t), w - w_t \rangle_{\mathcal{W}} + \alpha_t D_\Omega(w \parallel w_t), \quad (6)$$

where $\alpha_t := 1/\eta_t$ denotes an inverse of the current step size η_t [46]. Plugging each divergence of the cumulative cost F_t to Eq. (6), the MD-IRL update for the subsequent reward function $\psi_{t+1} = \Psi_\Omega(\pi_{t+1})$ is derived by solving a problem

$$\begin{aligned} & \underset{\pi^s \in \Pi^s}{\text{minimize}} \underbrace{\langle \nabla D_\Omega(\pi_t^s \parallel \bar{\pi}_{E,t}^s), \pi^s - \pi_t^s \rangle_{\mathcal{A}}}_{\nabla \Omega(\pi_t^s) - \nabla \Omega(\bar{\pi}_{E,t}^s)} + \alpha_t D_\Omega(\pi^s \parallel \pi_t^s) \\ \iff & \underset{\pi^s \in \Pi^s}{\text{minimize}} D_\Omega(\pi^s \parallel \bar{\pi}_{E,t}^s) - D_\Omega(\pi^s \parallel \pi_t^s) + \alpha_t D_\Omega(\pi^s \parallel \pi_t^s) \\ \iff & \underset{\pi^s \in \Pi^s}{\text{minimize}} \eta_t \underbrace{D_\Omega(\pi^s \parallel \bar{\pi}_{E,t}^s)}_{\text{estimated expert}} + (1 - \eta_t) \underbrace{D_\Omega(\pi^s \parallel \pi_t^s)}_{\text{learning agent}} \quad \forall s \in \mathcal{S}, \end{aligned} \quad (7)$$

where the gradient of D_Ω is taken with respect to its first argument π_t^s . Note that solving the optimization Eq. (7) requires interaction between π_t and the dynamics of the given environment in order to minimize F_t ; thus, the corresponding RL process plays an essential role in sequential learning by the induced the value measures. At a glance, the objective is analogous to finding an interpolation at each iteration where the point is controlled η_t . Fig. 3 shows that the uncertainty of π_t (blue region) gets minimal regardless of persisting uncertainty of $\bar{\pi}_{E,t}$ (red region).

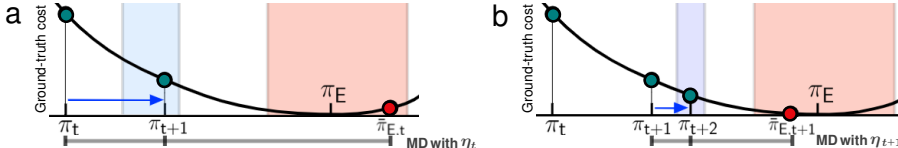


Figure 3: Illustrations of MD at the (a) t -th iteration and (b) $(t+1)$ -th iteration where $\eta_t > \eta_{t+1}$. $\{\bar{\pi}_{E,t}\}_{t=1}^\infty$ is an arbitrary estimation process attained from a neighborhood of π_E with respect to a norm. The MD update is taken inside the interval of π_t and $\bar{\pi}_{E,t}$ using Eq. (7).

5 Convergence Analyses

In this section, we present our theoretical results. The main goals of the following arguments are to address ① the convergence of MD updates for various cases and ② the necessity of scheduling the amount of learning. Suppose that state instances of $s_i^{(t)} \in \tau_t$ cover the entire \mathcal{S} by executing the policy π_t in an infinite horizon. From this assumption, we define a temporal cost function at the time step t :

$$f(\pi_t, \tau_t) := \sum_{i=0}^{\infty} \gamma^i D_\Omega(\pi_t(\cdot \mid s_i^{(t)}) \parallel \bar{\pi}_{E,t}(\cdot \mid s_i^{(t)})), \quad (8)$$

that involves π_t , and additionally a trajectory τ_t as inputs. We refer to the global objective as finding a unique fixed point $\pi_* \in \Pi$ that minimizes a total cost $F(\pi) := \mathbb{E}[f(\pi, \tau_t)]$, where the expectation is taken over trajectories of entire steps, i.e., $\lim_{t \rightarrow \infty} \mathbb{E}_{\tau_{1:t}}[f(\pi, \tau_t)]$. Taking the (stepwise) gradient for each $\pi(\cdot \mid s)$, an optimal policy π_* is found by $\mathbb{E}[\nabla \Omega(\pi_*(\cdot \mid s)) - \nabla \Omega(\bar{\pi}_{E,t}(\cdot \mid s))] = 0$ when $t \rightarrow \infty$; hence, $\nabla \Omega(\pi_*(\cdot \mid s)) = \lim_{t \rightarrow \infty} \mathbb{E}[\nabla \Omega(\bar{\pi}_{E,t}(\cdot \mid s))]$. Introducing the optimal policy π_* allows not only the specific situation when ① $\pi_E = \pi_* \in \Pi$ and the estimation algorithm of $\bar{\pi}_{E,t}$ is actually convergent with $t \rightarrow \infty$, but also more general situations where ② $\pi_E \notin \Pi$ or the estimated expert policy $\bar{\pi}_{E,t}$ does not converge; the algorithm finds convergence to a fixed point by scheduling updates.

We state two conditions of $\{\eta_t\}_{t=1}^\infty$ to guarantee convergence justified in Theorems 1 and 2.

- Convergent sequence & divergent series:

$$\lim_{t \rightarrow \infty} \eta_t = 0 \quad \text{and} \quad \sum_{t=1}^\infty \eta_t = \infty. \quad (9)$$

- Divergent series & convergent series of squared terms:

$$\sum_{t=1}^\infty \eta_t = \infty \quad \text{and} \quad \sum_{t=1}^\infty \eta_t^2 < \infty. \quad (10)$$

Let us assume Lipschitz continuity of $\nabla \Omega$ and boundedness of D_Ω in a Banach space. In some Ω , these two assumptions do not necessarily hold for extreme cases in $\Delta_{\mathcal{A}}^S$, e.g., a distribution that $\pi(a|s) = 0$ for some entries. Nevertheless, these outliers can be left out if the parametrization is constrained to satisfy the assumptions. For example, one can either ① prevent a policy from having non-zero entries of probabilities for a discrete policy or ② prevent a policy from having too low entropy for a continuous policy, by enforcing certain constraints on its parametric representations.

Theorem 1 argues that the sequence $\{\eta_t\}_{t=1}^\infty$ shall diverge for its series; therefore, Eq. (9) is satisfied.

Theorem 1 (Stepsize considerations). *Let Ω be strongly convex, $\nabla \Omega$ be Lipschitz continuous, and the associated Bregman divergence D_Ω is bounded. Assume a general condition of the problem that $\inf_{\pi \in \Pi} \mathbb{E}[f(\pi, \tau_t)] > 0$. Then we get $\lim_{T \rightarrow \infty} \mathbb{E}_{\tau_1:T} [\sum_{i=0}^\infty D_\Omega(\pi_*(\cdot|s_i) \|\pi_T(\cdot|s_i))] = 0$ if and only if Eq. (9) is satisfied.*

- (a) *If $\lim_{t \rightarrow \infty} \eta_t = 0$, then $T \in \mathbb{N}$, $n < T$, and $c > 0$ exist such that $\mathbb{E}_{\tau_1:T} [f_T(\pi_T, \tau_T)] \geq \frac{c}{T-n}$.*
- (b) *If the step size is in the form of $\eta_t = \frac{4}{t+1}$, then $\mathbb{E}_{\tau_1:T} [\sum_{i=0}^\infty D_\Omega(\pi_*(\cdot|s_i) \|\pi_T(\cdot|s_i))] = \mathcal{O}(1/T)$.*

Next, we present Theorem 2, which addresses the convergence in a specific case when π_E resides in Π . Additionally, the theorem addresses the bounds of the performance for fixed size update $\eta_t \equiv \eta_1$.

Theorem 2 (Optimal cases). *Let Ω be strongly convex, $\nabla \Omega$ be Lipschitz continuous, and the associated Bregman divergences be bounded. Assume $\pi_1 \neq \pi_E$ and $\inf_{\pi \in \Pi} \mathbb{E}[f(\pi, \tau_t)] = 0$. Then, $\mathbb{E}[f(\pi_t, \tau_t)] = 0$ if and only if $\sum_{t=1}^\infty \eta_t = \infty$. If $\eta_t \equiv \eta_1$, then there exist $c_1, c_2 \in (0, 1)$ such that $c_1^{T-1} \cdot A_1 \leq A_T \leq c_2^{T-1} \cdot A_1$, for $A_t = \sup_{s \in \mathcal{S}} \mathbb{E}_{\tau_1:t} [D_\Omega(\pi_E^s \|\pi_t^s)]$.*

Lastly, Proposition 1 provides the sufficient condition for the almost certain convergence of the algorithm by imposing the stronger condition of step size in Eq. (10). The proofs are in Appendix A.

Proposition 1 (General cases). *Assume that $\pi_E \notin \Pi$, hence $\inf_{\pi \in \Pi} \mathbb{E}[f(\pi, \tau_t)] > 0$. If the step sizes satisfies Eq. (10), then $\lim_{t \rightarrow \infty} \sum_{i=0}^\infty \gamma^i D_\Omega(\pi_*(\cdot|s_i) \|\pi_t(\cdot|s_i))$ converges to 0 almost surely.*

Regrets. For a sequence of state trajectories $\{\tau_t\}_{t \in \mathbb{N}}$, let us define a regret at the t -th iteration as

$$\frac{1}{t} \sum_{i=1}^t f(\pi_i, \tau_i) - \inf_{\pi \in \Pi} \left\{ \frac{1}{t} \sum_{j=1}^t f(\pi, \tau_j) \right\}. \quad (11)$$

In the optimal case of $\inf_{\pi \in \Pi} \mathbb{E}[f(\pi, \tau_t)] = 0$, the cost f inherits the property of Bregman divergence so that the infimum is achieved by 0 at π_E . In this case, the regret is bounded to $\mathcal{O}(1/T)$ by the theorems. By Proposition 1, the MD updates converge for the case of $\inf_{\pi \in \Pi} \mathbb{E}[f(\pi, \tau_t)] > 0$ when the step sizes abide by Eq. (10). Thus, the regret is bounded to $\mathcal{O}(1/T)$ even for the general case.

6 Algorithm: MD-IRL on an Adversarial Framework

In this section, we propose MD-AIRL, a novel AIL algorithm which trains a parameterized reward function with adversarial learning and the MD update rule. Neural network parameters θ , ϕ , and ν are newly presented representing agent policy, reward, and expert policy functions respectively.

Dual discriminators. In order to bridge the gap between theory and practice, we propose a novel discriminative architecture, motivated by GAN studies regarding multiple discriminators [47, 48]. Basically, the proposed discriminators separate two concepts in AIL: matching overall state densities and imitating specific behavior. Given a learning agent policy π_θ , an estimation policy π_ν , and a discriminative neural network for states $d_\xi : \mathcal{S} \rightarrow \mathbb{R}$, the two discriminators are defined as

$D_\nu(s, a; \theta, \xi) = \sigma(\log\{\pi_\nu(a|s)/\pi_\theta(a|s)\} + d_\xi(s))$ and $D_\xi(s) = \sigma(d_\xi(s))$, $\forall s \in \mathcal{S}, a \in \mathcal{A}$, where $\sigma(\cdot)$ denotes the sigmoid function. The discriminators are trained using binary logistic regression losses with respect to mini-batch adversarial samples:

$$\text{maximize } \mathcal{J}_{d_\xi} = \mathbb{E}_{\pi_E} [\log D_\xi(s)] + \mathbb{E}_{\pi_\theta} [\log(1 - D_\xi(s))], \quad (12)$$

$$\text{maximize } \mathcal{J}_{\pi_\nu} = \mathbb{E}_{\pi_E} [\log D_\nu(s, a)] + \mathbb{E}_{\pi_\theta} [\log(1 - D_\nu(s, a))], \quad (13)$$

Algorithm 1 Mirror Descent Adversarial Inverse Reinforcement Learning.

- 1: **Input:** trajectories $\{\tau_t^*\}_{t=1}^T$, an agent π_θ , a reference policy π_ν , a neural network $d_\xi: \mathcal{S} \rightarrow \mathbb{R}$, a regularized reward function $\psi_\phi \in \Psi_\Omega(\Pi)$, α_1, α_T , and λ .
- 2: **for** $t \leftarrow 1$ to T **do**
- 3: $\alpha_t \leftarrow \alpha_1 + (t-1)(\alpha_T - \alpha_1)/(T-1)$ and then $\eta_t \leftarrow 1/\alpha_t$.
- 4: Optimize d_ξ and π_ν via binary logistic regression for D_ξ and D_ν .
- 5: Optimize ψ_ϕ with the objective in Eq. (14) using both τ_t^* and τ_t .
- 6: Train π_θ via RL to maximize $\psi_\phi^\lambda(s, a)$ with regularizer $\lambda\Omega(\cdot)$.
- 7: **Output:** $\pi_\theta, \psi_\phi^\lambda$.

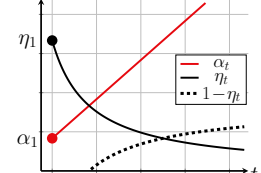


Figure 4: A sequence example of (α_t, η_t) .

where d_ξ and π_θ are not trained for learning D_ν . Let $\rho_\pi \in \Delta_{\mathcal{S}}$ denote the state visitation density of π , which is defined as $\rho_\pi(s) := (1-\gamma) \mathbb{E}_\pi \left[\sum_{i=0}^{\infty} \gamma^i \mathbb{I}\{s_i = s\} \right]$, where $\mathbb{I}\{\cdot\}$ is an indicator function. The convergence of functions in an ideal case is found at $\pi_\nu = \pi_E$ and $d_\xi(s) = \log\{\rho_{\pi_E}(s)/\rho_{\pi_\theta}(s)\}$.

Learning with MD-based rewards. Based on the MD solution for a regularized reward function, we focus on developing an MD-based learning objective. Let $\psi_\phi \in \Psi(\Pi)$ denote a parameterized regularized reward function, and π_ϕ denotes a corresponding policy from ϕ . Note that the transformation between ψ_ϕ and π_ϕ can be performed with shared ϕ without the additional computational costs under specific parameterizations [18]. Using a step size η_t , the RL agent π_θ , and the estimated expert policy π_ν , we define the objective of ϕ as a direct interpretation of the update rule of Eq. (7):

$$\text{minimize } \mathcal{L}_{\psi_\phi} = \mathbb{E}_{s \sim \bar{\tau}_t} [\eta_t D_\Omega(\pi_\phi(\cdot|s) \| \pi_\nu(\cdot|s)) + (1-\eta_t) D_\Omega(\pi_\phi(\cdot|s) \| \pi_\theta(\cdot|s))], \quad (14)$$

where the trajectory $\bar{\tau}_t$ denotes sample states using both agent and expert trajectories. As shown in Fig. 4, η_t is adjusted by linearly increasing α_t , which originated from the analyses in Section 5.

Another important consideration is the way of handling covariate shifts [49] since it is likely that state densities between the expert and the agent are misaligned. Thus, we define the IRL reward function as linear combinations of ψ_ϕ and the state density discriminative signal:

$$\psi_\phi^\lambda(s, a) = \lambda \psi_\phi(s, a) + d_\xi(s), \quad (15)$$

with a coefficient $\lambda \in \mathbb{R}^+$. Utilizing an arbitrary regularized RL algorithm with a regularizer $\lambda\Omega(\cdot)$, the reward learning regarding agent policy π_θ is decomposed into the following:

$$\begin{aligned} \mathbb{E}_{\pi_\theta} [\psi_\phi^\lambda(s, a) - \lambda\Omega(\pi_\theta(\cdot|s))] &= \lambda \mathbb{E}_{\pi_\theta} [\psi_\phi(s, a) - \Omega(\pi_\theta(\cdot|s))] - D_{\text{KL}}(\rho_{\pi_\theta} \| \rho_{\pi_E}) \\ &= -\lambda \mathbb{E}_{\pi_\theta} [D_\Omega(\pi_\theta(\cdot|s) \| \pi_\phi(\cdot|s))] - D_{\text{KL}}(\rho_{\pi_\theta} \| \rho_{\pi_E}). \end{aligned}$$

Minimizing the first term of $\mathbb{E}_{\pi_\theta} [D_\Omega(\pi_\theta^s \| \pi_\phi^s)]$ represents learning with the MD formulation. Minimizing the second term $D_{\text{KL}}(\rho_{\pi_\theta} \| \rho_{\pi_E})$ plays an auxiliary role in facilitating the supports of state visitation densities to be correctly matched. With the hyperparameter λ , we report that learning the second term is helpful when the state densities are heavily misaligned in certain benchmarks. Algorithm 1 summarizes the entire procedure. We defer additional details to Appendices B and C.

7 Experimental Results

The aim of our experiments was to identify whether MD-AIRL facilitates robustness for various Ω while retaining the scalability of AIL. The comparative method was RAIRL with density-based models (RAIRL-DBM) which contained comparable expressiveness as MD-AIRL. For RL, we used RAC [44], which is a generalization of the SAC algorithm [50]. We considered a class of regularizers $\Omega(p) = -\mathbb{E}_{x \sim p} [\varphi(p(x))]$ with ① Shannon ($\varphi(x) = \log(x)$), ② Tsallis ($\varphi(x; q) = \frac{1}{q-1}(x^{q-1} - 1)$, $q = 2$ by default), ③ exp ($\varphi(x) = e - e^x$), ④ cos ($\varphi(x) = \cos(\frac{\pi}{2}x)$), and ⑤ sin ($\varphi(x) = 1 - \sin(\frac{\pi}{2}x)$).

7.1 Large scale multiarmed bandits

To measure the performance of IRL, we first considered multiarmed bandit problems, where the cardinality of action spaces varies largely. Learning the optimal distribution of π_E becomes challenging as the cardinality of the space $|\mathcal{A}|$ increases, because the frequency of each sample becomes sparse due to the curse of dimensionality. The stateless expert distribution π_E was generated by the parameters of softmax distribution $\pi_E(a) = \exp(z_a)/\sum_i \exp(z_i)$, where the logits z_i were randomly initialized. We set the action size to $|\mathcal{A}| = 10^2, 10^3, 10^4$ and restricted each sample size of 16.

Table 2: The training results of $|\mathcal{A}| \cdot D_{\Omega}(\pi_T \| \pi_E)$ with five types of regularization (five runs with different seeds).

Method	$ \mathcal{A} = 10^2$		$ \mathcal{A} = 10^3$		$ \mathcal{A} = 10^4$	
	RAIRL	MD-AIRL	RAIRL	MD-AIRL	RAIRL	MD-AIRL
Shannon	2.55 ± 1.59	2.28 ± 1.20	140.3 ± 87.5	125.3 ± 61	-	-
Tsallis	0.21 ± 0.13	0.11 ± 0.04	0.55 ± 0.13	0.24 ± 0.03	4.95 ± 2.3	4.21 ± 0.2
exp	0.27 ± 0.17	0.18 ± 0.06	0.55 ± 0.12	0.23 ± 0.03	5.06 ± 2.4	4.97 ± 0.7
cos	0.05 ± 0.04	0.02 ± 0.01	0.03 ± 0.02	0.01 ± 0.01	0.21 ± 0.6	0.05 ± 0.1
sin	0.34 ± 0.25	0.12 ± 0.04	3.82 ± 3.46	1.07 ± 0.75	8.12 ± 3.8	7.59 ± 1.0

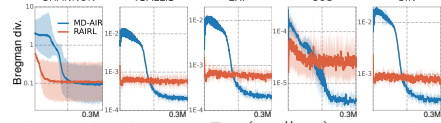


Figure 5: The cost $D_{\Omega}(\pi_T \| \pi_E)$ on the log scale at $|\mathcal{A}| = 10^3$. The shade represents 95% confidence interval.

Tab. 2 shows that MD-AIRL achieved overall lower Bregman divergence on average when three different cardinalities and five regularizers were considered. Fig. 5 shows that the Bregman divergence was large for MD-AIRL at the early training phase, because we chose the initial step size η_1 to be greater than 1 ($\alpha_1 = 0.5$). MD-AIRL exceeded the discriminative performance of RAIRL after certain steps, while the progression of RAIRL mostly stopped at local minima. MD-AIRL outperformed RAIRL in four cases by choosing an effectively low step size at η_T to be less than 1 ($\alpha_T = 2$). These results match the properties of MD algorithms and our convergence analyses. Therefore, we argue that a constrained update rule with appropriate step sizes is necessary for robust reward acquisition and imitation for situations when the total number of data samples is limited.

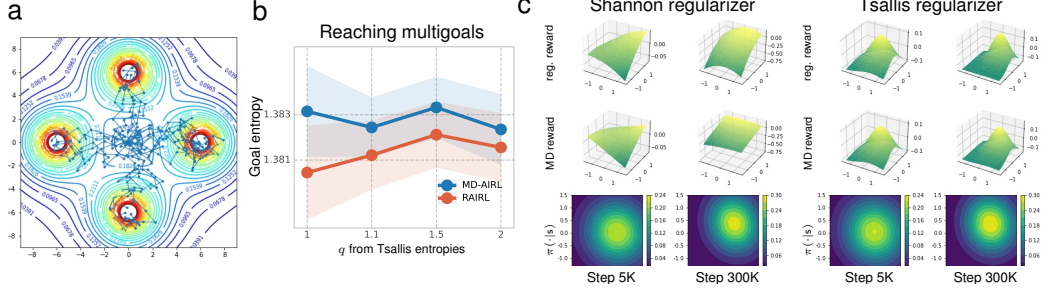


Figure 6: (a) Visualization of trajectories trained by MD-AIRL, and the ground-truth reward surface. (b) The entropies for the probabilities of achieving four goals. The x-axis indicates the q value from the Tsallis regularizers (the Shannon regularizer is considered by $q=1$ [51]). (c) The top and middle of each column show induced reward surfaces. The bottom shows the agent policy.

7.2 A continuous multigoal environment

We then considered a multigoal environment. In this environment, an agent is a two-dimensional point mass initialized at the origin, and the four goals are located in the four cardinal directions. The objective of imitation learning is to go toward each direction evenly as possible where the expert model was trained by the SAC algorithm. To draw informative reward surfaces regarding stochastic actions, we considered the multivariate Gaussian distribution policies parameterized with full covariance matrices instead of conventional diagonal Gaussian policies (see Appendices B and C).

Fig. 6 (a) shows trajectories generated by the trained agent. Fig. 6 (b) shows that MD-AIRL achieved higher entropy for reaching the multiple goals. Fig. 6 (c) shows reward surfaces with regularizers, which were calculated by $\psi_{\phi}(s, a) + \varphi(\pi_{\theta}(a|s))$ for each point of $a \in \mathcal{A}$ and $s = (5, -1)$. During the training, the MD reward was similar to the estimated ground truth using adversarial training. However, the surface of MD-AIRL became flatter than the ground-truth estimation when π_t was sufficiently close to the expert behavior. As a result, we claim that a drastic change in the target distribution, which is one of the typical characteristics of adversarial frameworks, is prevented. We argue that these characteristics mitigate overfitting caused by unreliable discriminative signals.

7.3 A continuous control benchmark: MuJoCo

Lastly, we validated MD-AIRL on the MuJoCo continuous control benchmark suite. We assumed full covariance Gaussian policies for both learner’s policy π and expert policy π_E . We used the hyperbolized environment assumption [18] where the action constraint is incorporated into the dynamics as a part of the environment using hyperbolic tangent activation.

Sample efficiency. For each task, we considered two different numbers of episodes collected by an expert policy. In Fig. 7, the performance of MD-AIRL, RAIRL, and behavior cloning (bc) algorithms [20] is shown with the expert and random agent performance. MD-AIRL was able

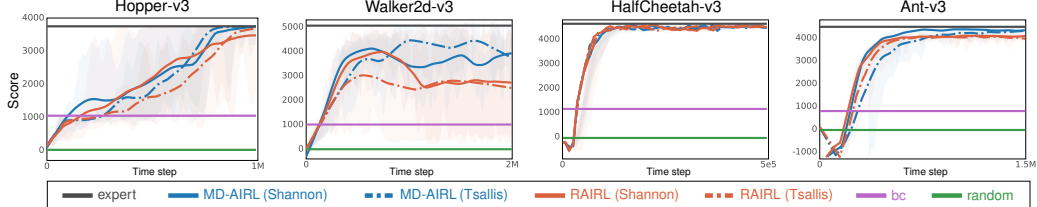


Figure 7: Average scores for 5 runs with two different regularizers (Shannon and Tsallis regularizer). The agent and IRL reward functions were trained with 4 episodes of expert demonstrations.

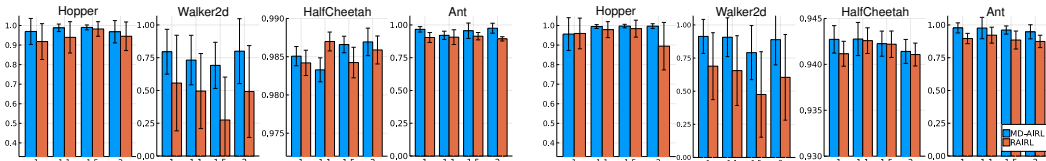


Figure 8: Scores on the last 10^5 steps in a total of 32 different settings. The x -axis indicates the q value of the Tsallis regularizers. The scores are rescaled by considering the expert performance as 1, and the error bars represent standard deviations. Left: 4 demonstrations. Right: 100 demonstrations.

to achieve consistent performance throughout the tasks and demonstration size. On the training curves, MD-AIRL showed high tolerance to the scarcity of data compared to RAIRL for 4 expert demonstrations. The plots in Fig. 8 indicate that MD-AIRL showed higher average scores with lower variance compared to RAIRL, across 30 distinct cases among 32 configurations we have tested. MD-AIRL inherits the scalability of AIL, and it is highly stable with respect to limited sample sizes.

Table 3: Scores on noisy demonstrations. The values of ε represents scales of the Gaussian noises.

		$\varepsilon = 0.01$	$\varepsilon = 0.5$	$\varepsilon = 0.01$	$\varepsilon = 0.5$
Hopper	RAIRL (Shannon)	3636.03 \pm 391.09	3573.74 \pm 508.14	RAIRL (Shannon)	4354.15 \pm 63.83
	MD-AIRL (Shannon)	3669.25 \pm 177.78	3653.31 \pm 267.87	MD-AIRL (Shannon)	4373.17 \pm 68.12
	RAIRL (Tsallis)	3671.12 \pm 322.32	3576.17 \pm 515.75	RAIRL (Tsallis)	4364.13 \pm 68.09
	MD-AIRL (Tsallis)	3730.14 \pm 63.09	3701.24 \pm 205.68	MD-AIRL (Tsallis)	4388.87 \pm 73.19
Walker2d	RAIRL (Shannon)	2856.56 \pm 939.9	2451.00 \pm 1392.6	RAIRL (Shannon)	4493.74 \pm 383.04
	MD-AIRL (Shannon)	3386.38 \pm 953.59	3252.65 \pm 1395.7	MD-AIRL (Shannon)	4658.29 \pm 201.37
	RAIRL (Tsallis)	2731.84 \pm 1058.7	2435.10 \pm 1555.2	RAIRL (Tsallis)	4359.62 \pm 168.46
	MD-AIRL (Tsallis)	3624.00 \pm 992.63	3093.54 \pm 963.96	MD-AIRL (Tsallis)	4705.25 \pm 130.53
HalfCheetah	RAIRL (Shannon)	4354.15 \pm 63.83	4216.99 \pm 661.17	RAIRL (Shannon)	4354.15 \pm 63.83
	MD-AIRL (Shannon)	4373.17 \pm 68.12	4337.18 \pm 106.40	MD-AIRL (Shannon)	4373.17 \pm 68.12
	RAIRL (Tsallis)	4364.13 \pm 68.09	4216.67 \pm 248.08	RAIRL (Tsallis)	4364.13 \pm 68.09
	MD-AIRL (Tsallis)	4388.87 \pm 73.19	4247.44 \pm 266.73	MD-AIRL (Tsallis)	4388.87 \pm 73.19
Ant	RAIRL (Shannon)	3777.78 \pm 505.78	3660.22 \pm 508.54	RAIRL (Shannon)	4493.74 \pm 383.04
	MD-AIRL (Shannon)	4658.29 \pm 201.37	4284.38 \pm 329.79	MD-AIRL (Shannon)	4658.29 \pm 201.37
	RAIRL (Tsallis)	3660.22 \pm 508.54	3777.78 \pm 505.78	RAIRL (Tsallis)	4493.74 \pm 383.04
	MD-AIRL (Tsallis)	4705.25 \pm 130.53	4127.37 \pm 457.25	MD-AIRL (Tsallis)	4705.25 \pm 130.53

Noisy demonstrations. Tab. 3 shows the results of imitation learning experiments for 100 expert demonstrations with two levels of Gaussian additive noises, resulting in suboptimal demonstrations. MD-AIRL is highly tolerant to noisy data, consistently achieving higher performance. The experiment is closely related to the general case in the theory; the results suggest that the characteristics of MD-AIRL are in alignment with our analyses of the MD reward learning scheme.

We present a detailed analysis of the noisy demonstration experiments (Fig. 9). Let the Bregman divergence between agent and ground-truth expert policies be the error, and we measured these errors by increasing the given noise level for the expert trajectories. Fig. 9 shows a general tendency that MD-AIRL has lower errors than RAIRL. With Tab. 3 and Fig. 9, we were able to find the evident correlation between average Bregman divergence and performance since imitation learning converges when the divergence is zero. Thus, this is another piece of empirical evidence that verifies our theoretical claims.

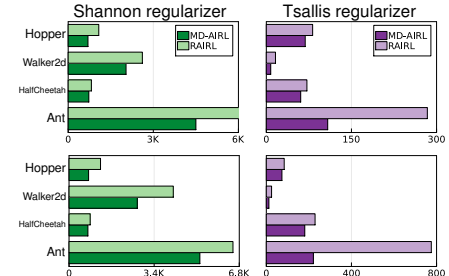


Figure 9: Divergences after imitation learning. Top: $\varepsilon = 0.01$. Bottom: $\varepsilon = 0.5$.

8 Conclusions and Discussion

In this paper, we presented MD-AIRL, a practical AIL algorithm designed to solve the imitation learning problem in the real world. We proved that the proposed method has clear advantages over previous AIL methods in terms of robustness. We verified MD-AIRL in a variety of situations, including high-dimensional spaces, limited samples, and imperfect demonstrations. The empirical

evidence showed that MD-AIRL outperforms previous methods on various benchmarks. We conclude that the rich foundation of optimization theories shows a promising direction for AIL studies.

Considering RL and IRL with geometric perspectives is vital for solving real-world problems. Although our work covers various imitation learning problems with the Bregman divergence, this does not include some other problems when the proximity term is of other statistical divergence families, such as the f-divergence [52]. If the relationship between these classes of divergences is studied in more detail, it is expected to proceed with applications to various subfields of machine learning. The assumptions on Ω in our analyses are usually justified by enforcing a specific policy space, but some outliers might have substantial meaning for certain tasks. Therefore, extensive analyses on these parameterizations remain as future works. The “impurity” of the MD-AIRL reward function compared to $\Psi_\Omega(\Pi)$ can be regarded as a limitation. To fully resolve this problem, all data must be treated as on-policy samples, which might require a sophisticated sampling mechanism.

Societal impacts. The evolution of imitation learning algorithms is expected to bring a structural shift in the labor market. The negative impact could be mitigated by diversification, unification, and redefinition of routine and manual jobs. The results of our work can be abused as a tool for analyzing individual data. Therefore, we stress that certain acts should be carefully regulated, such as collecting a substantial amount of individuals’ data and aggressively tracking personal identity.

Acknowledgments

The authors would like to thank the anonymous reviewers, Woosuk Choi, Jaein Kim, and Min Whoo Lee for their helpful discussion and comments. This work was partly supported by the IITP (2022-0-00951-LBA/25%, 2022-0-00953-PICA/25%, 2015-0-00310-SW.StarLab/10%, 2021-0-02068-AIHub/10%, 2021-0-01343-GSAI/10%, 2019-0-01371-BabyMind/10%) grant funded by the Korean government, and the CARAI (UD190031RD/10%) grant funded by the DAPA and ADD.

References

- [1] Ziyu Wang, Josh S Merel, Scott E Reed, Nando de Freitas, Gregory Wayne, and Nicolas Heess. Robust imitation of diverse behaviors. In I. Guyon, U. V. Luxburg, S. Bengio, H. Wallach, R. Fergus, S. Vishwanathan, and R. Garnett, editors, *Advances in Neural Information Processing Systems*, volume 30, 2017.
- [2] Yuke Zhu, Ziyu Wang, Josh Merel, Andrei Rusu, Tom Erez, Serkan Cabi, Saran Tunyasuvunakool, János Kramár, Raia Hadsell, Nando de Freitas, and Nicolas Heess. Reinforcement and imitation learning for diverse visuomotor skills. In *Proceedings of Robotics: Science and Systems*, 2018.
- [3] Beomjoon Kim, Amir-massoud Farahmand, Joelle Pineau, and Doina Precup. Learning from limited demonstrations. In *Advances in Neural Information Processing Systems*, volume 26, 2013.
- [4] Andrew Y Ng and Stuart J Russell. Algorithms for inverse reinforcement learning. In *Proceedings of the 17th International Conference on Machine Learning*, pages 663–670. Morgan Kaufmann Publishers Inc., 2000.
- [5] Robert Dadashi, Léonard Hussenot, Matthieu Geist, and Olivier Pietquin. Primal wasserstein imitation learning. In *9th International Conference on Learning Representations*, 2021.
- [6] Pieter Abbeel and Andrew Y Ng. Apprenticeship learning via inverse reinforcement learning. In *Proceedings of the 21st International Conference on Machine Learning*, page 1. ACM, 2004.
- [7] Brian D Ziebart, Andrew Maas, J Andrew Bagnell, and Anind K Dey. Maximum entropy inverse reinforcement learning. In *Proceedings of 23rd AAAI Conference on Artificial Intelligence*, volume 3, pages 1433–1438, 2008.
- [8] Richard S. Sutton and Andrew G. Barto. *Reinforcement Learning: An Introduction*. The MIT Press, second edition, 2018.
- [9] Jonathan Ho and Stefano Ermon. Generative adversarial imitation learning. In *Advances in Neural Information Processing Systems*, pages 4565–4573, 2016.
- [10] Justin Fu, Katie Luo, and Sergey Levine. Learning robust rewards with adversarial inverse reinforcement learning. *arXiv preprint arXiv:1710.11248*, 2017.

[11] Ian Goodfellow, Jean Pouget-Abadie, Mehdi Mirza, Bing Xu, David Warde-Farley, Sherjil Ozair, Aaron Courville, and Yoshua Bengio. Generative adversarial nets. In *Advances in Neural Information Processing Systems*, pages 2672–2680, 2014.

[12] Ilya Kostrikov, Kumar Krishna Agrawal, Debidatta Dwibedi, Sergey Levine, and Jonathan Tompson. Discriminator-actor-critic: Addressing sample inefficiency and reward bias in adversarial imitation learning. In *7th International Conference on Learning Representations*, 2019.

[13] Seyed Kamayr Seyed Ghasemipour, Richard Zemel, and Shixiang Gu. A divergence minimization perspective on imitation learning methods. In *Conference on Robot Learning*, pages 1259–1277. PMLR, 2020.

[14] Dan Butnariu and Elena Resmerita. Bregman distances, totally convex functions, and a method for solving operator equations in banach spaces. In *Abstract and Applied Analysis*, volume 2006, 2006.

[15] Arkadii Semenovich Nemirovsky and David Borisovich Yudin. *Problem Complexity and Method Efficiency in Optimization*. A Wiley-Interscience publication. Wiley, 1983. ISBN 9780471103455.

[16] Nati Srebro, Karthik Sridharan, and Ambuj Tewari. On the universality of online mirror descent. In *Advances in Neural Information Processing Systems*, pages 2645–2653, 2011.

[17] Yunwen Lei and Ding-Xuan Zhou. Convergence of online mirror descent. *Applied and Computational Harmonic Analysis*, 48(1):343 – 373, 2020. ISSN 1063-5203.

[18] Wonseok Jeon, Chen-Yang Su, Paul Barde, Thang Doan, Derek Nowrouzezahrai, and Joelle Pineau. Regularized inverse reinforcement learning. In *9th International Conference on Learning Representations*, 2021.

[19] Emanuel Todorov, Tom Erez, and Yuval Tassa. Mujoco: A physics engine for model-based control. In *2012 IEEE/RSJ International Conference on Intelligent Robots and Systems*, pages 5026–5033. IEEE, 2012.

[20] Dean A Pomerleau. Efficient training of artificial neural networks for autonomous navigation. *Neural computation*, 3(1):88–97, 1991.

[21] Lev M. Bregman. The relaxation method of finding the common point of convex sets and its application to the solution of problems in convex programming. *USSR computational mathematics and mathematical physics*, 7(3):200–217, 1967.

[22] Stephen P. Boyd and Lieven Vandenberghe. *Convex Optimization*. Cambridge University Press, 2014. ISBN 978-0-521-83378-3.

[23] Jean-Baptiste Hiriart-Urruty and Claude Lemaréchal. *Fundamentals of convex analysis*. Springer Science & Business Media, 2004.

[24] Arindam Banerjee, Srujana Merugu, Inderjit S. Dhillon, and Joydeep Ghosh. Clustering with bregman divergences. *Journal of Machine Learning Research*, 6(58):1705–1749, 2005.

[25] Akash Srivastava, Kristjan H. Greenewald, and Farzaneh Mirzazadeh. Bregmn: scaled-bregman generative modeling networks. *CoRR*, abs/1906.00313, 2019.

[26] Sreangsu Acharyya, Arindam Banerjee, and Daniel Boley. Bregman divergences and triangle inequality. In *Proceedings of the 13th International Conference on Data Mining*, pages 476–484, 2013.

[27] Shun-ichi Amari. Natural gradient works efficiently in learning. *Neural computation*, 10(2):251–276, 1998.

[28] G. Raskutti and S. Mukherjee. The information geometry of mirror descent. *IEEE Transactions on Information Theory*, 61(3):1451–1457, 2015.

[29] Manfredo P Do Carmo. *Differential geometry of curves and surfaces: revised and updated second edition*. Courier Dover Publications, 2016.

[30] Suriya Gunasekar, Blake E. Woodworth, and Nathan Srebro. Mirrorless mirror descent: A more natural discretization of riemannian gradient flow. *CoRR*, abs/2004.01025, 2020.

[31] Guanghui Lan. Policy mirror descent for reinforcement learning: Linear convergence, new sampling complexity, and generalized problem classes. *CoRR*, abs/2102.00135, 2021.

[32] Wenhao Zhan, Shicong Cen, Baihe Huang, Yuxin Chen, Jason D. Lee, and Yuejie Chi. Policy mirror descent for regularized reinforcement learning: A generalized framework with linear convergence. *CoRR*, abs/2105.11066, 2021.

[33] Manan Tomar, Lior Shani, Yonathan Efroni, and Mohammad Ghavamzadeh. Mirror descent policy optimization. *arXiv preprint arXiv:2005.09814*, 2020.

[34] Shun-ichi Amari. *Information geometry and its applications*, volume 194. Springer, 2016.

[35] Deepak Ramachandran and Eyal Amir. Bayesian inverse reinforcement learning. In *Proceedings of International Joint Conference on Artificial Intelligence*, pages 2586–2591, 2007.

[36] Gergely Neu and Csaba Szepesvári. Apprenticeship learning using inverse reinforcement learning and gradient methods. In *Proceedings of the 23rd Conference on Uncertainty in Artificial Intelligence*, pages 295–302, 2007.

[37] Monica Babes-Vroman, Vukosi Marivate, Kaushik Subramanian, and Michael Littman. Apprenticeship learning about multiple intentions. In *Proceedings of the 28th International Conference on International Conference on Machine Learning*, page 897–904, 2011. ISBN 9781450306195.

[38] Brian D Ziebart, J Andrew Bagnell, and Anind K Dey. Modeling interaction via the principle of maximum causal entropy. In *Proceedings of the 27th International Conference on International Conference on Machine Learning*, pages 1255–1262, 2010.

[39] Junbo Jake Zhao, Michaël Mathieu, and Yann LeCun. Energy-based generative adversarial networks. In *5th International Conference on Learning Representations*, 2017.

[40] Kyungjae Lee, Sungjoon Choi, and Songhwai Oh. Maximum causal tsallis entropy imitation learning. In *Advances in Neural Information Processing Systems*, pages 4403–4413, 2018.

[41] Amos Fiat and Gerhard J Woeginger. *Online algorithms: The state of the art*, volume 1442. Springer, 1998.

[42] Amir Beck and Marc Teboulle. Mirror descent and nonlinear projected subgradient methods for convex optimization. *Operations Research Letters*, 31(3):167–175, 2003.

[43] Matthieu Geist, Bruno Scherrer, and Olivier Pietquin. A theory of regularized Markov decision processes. In *Proceedings of the 36th International Conference on Machine Learning*, volume 97 of *Proceedings of Machine Learning Research*, pages 2160–2169. PMLR, 2019.

[44] Wenhao Yang, Xiang Li, and Zhihua Zhang. A regularized approach to sparse optimal policy in reinforcement learning. In *Advances in Neural Information Processing Systems*, pages 5938–5948, 2019.

[45] Amir Beck and Marc Teboulle. Mirror descent and nonlinear projected subgradient methods for convex optimization. *Operations Research Letters*, 31(3):167–175, 2003. ISSN 0167-6377.

[46] David H Gutman and Javier F Peña. A unified framework for bregman proximal methods: subgradient, gradient, and accelerated gradient schemes. *arXiv*, pages arXiv–1812, 2018.

[47] Tu Nguyen, Trung Le, Hung Vu, and Dinh Phung. Dual discriminator generative adversarial nets. In I. Guyon, U. V. Luxburg, S. Bengio, H. Wallach, R. Fergus, S. Vishwanathan, and R. Garnett, editors, *Advances in Neural Information Processing Systems*, volume 30, 2017.

[48] LI Chongxuan, Taufik Xu, Jun Zhu, and Bo Zhang. Triple generative adversarial nets. In *Advances in Neural Information Processing Systems*, pages 4088–4098, 2017.

[49] Jonathan Chang, Masatoshi Uehara, Dhruv Sreenivas, Rahul Kidambi, and Wen Sun. Mitigating covariate shift in imitation learning via offline data with partial coverage. In *Advances in Neural Information Processing Systems*, volume 34, pages 965–979, 2021.

[50] Tuomas Haarnoja, Aurick Zhou, Pieter Abbeel, and Sergey Levine. Soft actor-critic: Off-policy maximum entropy deep reinforcement learning with a stochastic actor. In *International Conference on Machine Learning*, pages 1856–1865, 2018.

[51] Constantino Tsallis. Possible generalization of boltzmann-gibbs statistics. *Journal of statistical physics*, 52(1-2):479–487, 1988.

[52] Tianwei Ni, Harshit S. Sikchi, Yufei Wang, Tejas Gupta, Lisa Lee, and Ben Eysenbach. F-IRL: inverse reinforcement learning via state marginal matching. In *Conference on Robot Learning*, volume 155, pages 529–551. PMLR, 2020.

- [53] Frank Nielsen and Richard Nock. On Rényi and Tsallis entropies and divergences for exponential families. *arXiv preprint arXiv:1105.3259*, 2011.
- [54] Mohsen Pourahmadi. Joint mean-covariance models with applications to longitudinal data: Unconstrained parameterisation. *Biometrika*, 86(3):677–690, 1999.
- [55] Tuomas Haarnoja, Aurick Zhou, Kristian Hartikainen, George Tucker, Sehoon Ha, Jie Tan, Vikash Kumar, Henry Zhu, Abhishek Gupta, Pieter Abbeel, and Sergey Levine. Soft actor-critic algorithms and applications. *CoRR*, abs/1812.05905, 2018.
- [56] Martín Abadi, Ashish Agarwal, Paul Barham, Eugene Brevdo, Zhifeng Chen, Craig Citro, Greg S Corrado, Andy Davis, Jeffrey Dean, Matthieu Devin, et al. Tensorflow: Large-scale machine learning on heterogeneous distributed systems. *arXiv preprint arXiv:1603.04467*, 2016.

Appendices for
Robust Imitation via Mirror Descent Inverse Reinforcement Learning

A Proofs

We denote the entire set of conditional distributions as $\Delta_{\mathcal{A}}^{\mathcal{S}}$, which is a vector space formed by a collection of $|\mathcal{S}|$ elements of unit $(|\mathcal{A}| - 1)$ -simplexes: $\Delta_{\mathcal{A}} = \{ x_1 e_1 + \cdots + x_{|\mathcal{A}|} e_{|\mathcal{A}|} \mid \sum_{i=1}^{|\mathcal{A}|} x_i = 1 \text{ and } x_i \geq 0 \text{ for } i \in \mathcal{A} \}$. A trainable policy space is a subset of the entire conditional probability denoted as $\Pi := [\Pi^s]_{s \in \mathcal{S}} \subset \Delta_{\mathcal{A}}^{\mathcal{S}}$. We assume that Π^s is a member of a specific Banach space called L^p space $(\mathbb{R}^{\mathcal{A}}, \|\cdot\|)$, where $\|\cdot\|$ is a p -norm on \mathcal{A} . The dual space of L^p space for $1 < p < \infty$ is L^q space $(\mathbb{R}^{\mathcal{A}}, \|\cdot\|_*)$, where $\|\cdot\|_*$ is defined as a q -norm ($1/p + 1/q = 1$). Here, the condition $1 < p \leq 2$ is assumed for existence and convergence properties in the dual L^q space.

We begin with the following preliminary definitions: the Lipschitz continuity and martingales.

Definition 2 (Lipschitz constants). Given two metric spaces (X, d_X) and (Y, d_Y) where d_X denotes the metric on set X and d_Y is the metric on set Y , a function $f : X \rightarrow Y$ is called Lipschitz continuous if there exists a real constant $k \geq 0$ such that, for all x_1 and x_2 in X ,

$$d_Y(f(x_1), f(x_2)) \leq k \cdot d_X(x_1, x_2). \quad (16)$$

In particular, a function f is called Lipschitz continuous if there exists a constant $k \geq 0$ such that,

$$\|f(x_1) - f(x_2)\|_* \leq k \|x_1 - x_2\|, \quad \forall x_1, x_2 \quad (17)$$

where norms $\|\cdot\|$ and $\|\cdot\|_*$ are endowed with spaces X and Y respectively. For the smallest L that substitutes k , L is called the Lipschitz constant and f is called a L -Lipschitz continuous function.

Definition 3 (Discrete-time martingales). If a stochastic process $\{Z_t\}_{t \geq 1}$ satisfies $\mathbb{E}[|Z_n|] \leq \infty$ and

① $\mathbb{E}[Z_{n+1}|X_1, \dots, X_n] \leq Z_n$, ② $\mathbb{E}[Z_{n+1}|X_1, \dots, X_n] = Z_n$, ③ $\mathbb{E}[Z_{n+1}|X_1, \dots, X_n] \geq Z_n$.

Then, the stochastic process $\{Z_t\}_{t \geq 1}$ is called ① a submartingale, ② a martingale, and ③ a supermartingale, with respect to filtration $\{X_t\}_{t \geq 1}$.

The following arguments and proofs follow the results that appeared in previous literature for general aspects [15, 16, 42, 28, 17, 30]. Our analyses extend existing theoretical results to imitation learning and IRL; they are also highly general to cover various online methods for sequential decision problems.

A.1 Proof of Lemma 1

Proof of Lemma 1. The conjugate operator of ψ_{π}^s satisfies the following identity (Lemma 1 of [18])

$$\begin{aligned} \Omega^*(\psi_{\pi}^s) &= \max_{\tilde{\pi}^s \in \Delta_{\mathcal{A}}} \langle \tilde{\pi}^s, \psi_{\pi}^s \rangle_{\mathcal{A}} - \Omega(\tilde{\pi}^s) \\ &= \max_{\tilde{\pi}^s \in \Delta_{\mathcal{A}}} \langle \tilde{\pi}^s, \nabla \Omega(\pi^s) \rangle_{\mathcal{A}} - \langle \pi^s, \nabla \Omega(\pi^s) \rangle_{\mathcal{A}} + \Omega(\pi^s) - \Omega(\tilde{\pi}^s) \\ &= \min_{\tilde{\pi}^s \in \Delta_{\mathcal{A}}} \Omega(\tilde{\pi}^s) - \Omega(\pi^s) - \langle \nabla \Omega(\pi^s), \tilde{\pi}^s - \pi^s \rangle_{\mathcal{A}} \\ &= \min_{\tilde{\pi}^s \in \Delta_{\mathcal{A}}} D_{\Omega}(\tilde{\pi}^s \parallel \pi^s), \end{aligned}$$

for every state $s \in \mathcal{S}$. By the property of Bregman divergence and the convexity of $D_{\Omega}(\tilde{\pi}^s \parallel \pi^s)$ with respect to $\tilde{\pi}^s$, the optimal condition is obtained by the unique maximizing argument $\tilde{\pi}(\cdot|s) = \pi(\cdot|s)$. By taking gradient to both sides with respect to ψ_{π}^s we yield $\pi^s = \nabla \Omega^*(\psi_{\pi}^s)$.

If there is another $\tilde{\pi} \in \Delta_{\mathcal{A}}^{\mathcal{S}}$ that makes $\psi_{\tilde{\pi}} = \psi_{\pi}$, this contradicts the property of unique maximizing arguments for conjugates since $\pi \in \Pi$ and $\Pi \subset \Delta_{\mathcal{A}}^{\mathcal{S}}$. Therefore, ψ_{π} is uniquely defined for each π and $\nabla \Omega^*(\psi^s) \in \Pi^s$ for all $s \in \mathcal{S}$. \square

A.2 Proof of Theorem 1

Consider the unique fixed point of π_* as the solution of $\inf_{\pi \in \Pi} \mathbb{E}[f(\pi, \tau_t)]$ where the expectation indicates that we consider all outputs with respect to τ_t for $t \rightarrow \infty$ i.e., $\lim_{t \rightarrow \infty} \mathbb{E}_{\tau_{1:t}}[f(\pi, \tau_t)]$. By equating derivatives to zero, we write the condition of fixed point π_* as $\nabla \Omega(\pi_*) = \lim_{t \rightarrow \infty} \mathbb{E}[\nabla \Omega(\bar{\pi}_{E,t})]$. This assumption is useful since this paper provides some general results, the case of $\inf_{\pi \in \Pi} \mathbb{E}[f(\pi, \tau_t)] > 0$ in particular, which means that the estimates $\{\bar{\pi}_{E,t}\}_{t=1}^\infty$ do not converge to the fixed point of π_* , hence $\lim_{t \rightarrow \infty} \mathbb{E}_{\tau_{1:t}}[\|\pi_* - \bar{\pi}_{E,t}\|] \neq 0$. As a result, MD-based imitation learning algorithms allow many challenging settings, such as scarcity of data or imperfect demonstrations.

We first introduce a fundamental relationship regarding cumulative gradients in our online MD setting.

Lemma 2. *Let $\{\pi_t\}_{t=1}^\infty$, $\{\bar{\pi}_{E,t}\}_{t=1}^\infty$, and $\{\eta_t\}_{t=1}^\infty$ be policy, estimate, and step size sequences, respectively. The subsequent policy π_{t+1} in Eq. (7) is obtained by an RL algorithm using the derivation of ψ_{t+1} in Eq. (7), resulting to the following equation:*

$$\pi_{t+1}(\cdot | s) = \operatorname{argmin}_{\pi^s \in \Pi^s} \eta_t D_\Omega(\pi^s \| \bar{\pi}_{E,t}^s) + (1 - \eta_t) D_\Omega(\pi^s \| \pi_t^s) \quad \forall s \in \mathcal{S}. \quad (18)$$

We have for $t \in \mathbb{N}$,

$$\eta_t (\nabla \Omega(\pi_t^s) - \nabla \Omega(\bar{\pi}_{E,t}^s)) = \nabla \Omega(\pi_t^s) - \nabla \Omega(\pi_{t+1}^s) \quad \forall s \in \mathcal{S}. \quad (19)$$

Proof of Lemma 2. Since the optimization problem is convex with respect to each π^s , we equate the derivatives at π_{t+1} to zero:

$$\eta_t (\nabla \Omega(\pi_{t+1}^s) - \nabla \Omega(\bar{\pi}_{E,t}^s)) + (1 - \eta_t) (\nabla \Omega(\pi_{t+1}^s) - \nabla \Omega(\pi_t^s)) = 0, \quad \forall s \in \mathcal{S}.$$

Then, we derive Eq. (19) as

$$\begin{aligned} & \eta_t (\nabla \Omega(\pi_{t+1}^s) - \nabla \Omega(\bar{\pi}_{E,t}^s)) + (1 - \eta_t) (\nabla \Omega(\pi_{t+1}^s) - \nabla \Omega(\pi_t^s)) = 0 \\ \Leftrightarrow & \nabla \Omega(\pi_{t+1}^s) - \eta_t \nabla \Omega(\bar{\pi}_{E,t}^s) - (1 - \eta_t) \nabla \Omega(\pi_t^s) = 0 \\ \Leftrightarrow & \nabla \Omega(\pi_t^s) - \nabla \Omega(\pi_{t+1}^s) = \eta_t (\nabla \Omega(\pi_t^s) - \nabla \Omega(\bar{\pi}_{E,t}^s)) \quad \forall s \in \mathcal{S}. \end{aligned}$$

Therefore, the proof is complete. \square

Lemma 2 indicates that the distances between dual maps are equivalent to $\eta_t \|\nabla \Omega(\bar{\pi}_{E,t}^s) - \nabla \Omega(\pi_t^s)\|_*$. Therefore, when the step size converges as $\lim_{t \rightarrow \infty} \eta_t = 0$, the convergence in the dual space is induced as $\lim_{t \rightarrow \infty} \|\nabla \Omega(\pi_t^s) - \nabla \Omega(\pi_{t+1}^s)\|_* = 0$; thus, the convergence of associated reward functions for every state in Section 4 is reasonable when Ω is strongly smooth.

In the following lemmas (Lemmas 3-5), we omit the given state for simplicity since they hold for $\forall s \in \mathcal{S}$, hence one can write distributions $\pi_a = \pi_a^s$, $\pi_b = \pi_b^s$, and $\pi_c = \pi_c^s$ for a arbitrary given state s . First, we reintroduce the three-point identity as follows.

Lemma 3 (Three-point identity). *Let π_a , π_b , and π_c be any policy distributions with a given state. We have the following identity:*

$$\langle \nabla \Omega(\pi_a) - \nabla \Omega(\pi_b), \pi_c - \pi_b \rangle_{\mathcal{A}} = D_\Omega(\pi_c \| \pi_b) - D_\Omega(\pi_c \| \pi_a) + D_\Omega(\pi_b \| \pi_a)$$

Proof of Lemma 3. This can be derived using the definition of divergence as follows.

$$\begin{aligned} D_\Omega(\pi_c \| \pi_b) - D_\Omega(\pi_c \| \pi_a) + D_\Omega(\pi_b \| \pi_a) &= \Omega(\pi_c) - \Omega(\pi_b) - \langle \nabla \Omega(\pi_b), \pi_c - \pi_b \rangle_{\mathcal{A}} \\ &\quad - \Omega(\pi_c) + \Omega(\pi_a) + \langle \nabla \Omega(\pi_a), \pi_c - \pi_a \rangle_{\mathcal{A}} \\ &\quad + \Omega(\pi_b) - \Omega(\pi_a) - \langle \nabla \Omega(\pi_a), \pi_b - \pi_a \rangle_{\mathcal{A}} \\ &= \langle \nabla \Omega(\pi_a) - \nabla \Omega(\pi_b), \pi_c - \pi_b \rangle_{\mathcal{A}}. \end{aligned}$$

Therefore, the proof is complete. \square

Then, we introduce two identities in Lemmas 4 and 5 that are later used to address the progress of mirror descent updates in terms of Bregman divergences.

Lemma 4. *Let π_a , π_b , and π_c be any policy distributions with a given state. The following identity holds.*

$$D_\Omega(\pi_c\|\pi_b) - D_\Omega(\pi_c\|\pi_a) = D_\Omega(\pi_a\|\pi_b) + \langle \nabla\Omega(\pi_a) - \nabla\Omega(\pi_b), \pi_c - \pi_a \rangle_{\mathcal{A}} \quad (20)$$

Proof of Lemma 4. By Lemma 3, we have

$$D_\Omega(\pi_c\|\pi_b) - D_\Omega(\pi_c\|\pi_a) = -D_\Omega(\pi_b\|\pi_a) + \langle \nabla\Omega(\pi_a) - \nabla\Omega(\pi_b), \pi_c - \pi_b \rangle_{\mathcal{A}}.$$

Utilizing an identity of two Bregman divergences for arbitrary $(\pi, \tilde{\pi})$:

$$D_\Omega(\pi\|\tilde{\pi}) + D_\Omega(\tilde{\pi}\|\pi) = \langle \nabla\Omega(\pi) - \nabla\Omega(\tilde{\pi}), \pi - \tilde{\pi} \rangle_{\mathcal{A}}, \quad (21)$$

we separate $\pi_c - \pi_b$ into $\pi_c - \pi_a$ and $\pi_a - \pi_b$ and write the rest of the derivation as follows.

$$\begin{aligned} & D_\Omega(\pi_c\|\pi_b) - D_\Omega(\pi_c\|\pi_a) \\ &= \underbrace{-D_\Omega(\pi_b\|\pi_a) + \langle \nabla\Omega(\pi_a) - \nabla\Omega(\pi_b), \pi_a - \pi_b \rangle_{\mathcal{A}}}_{\text{Eq. (21)}} + \langle \nabla\Omega(\pi_a) - \nabla\Omega(\pi_b), \pi_c - \pi_a \rangle_{\mathcal{A}} \\ &= D_\Omega(\pi_a\|\pi_b) + \langle \nabla\Omega(\pi_a) - \nabla\Omega(\pi_b), \pi_c - \pi_a \rangle_{\mathcal{A}} \end{aligned}$$

Therefore, we achieve the desired identity. \square

Lemma 5. *Let π_a , π_b , and π_c be any policy distributions with a given state. The following identity holds.*

$$D_\Omega(\pi_b\|\pi_a) - D_\Omega(\pi_c\|\pi_a) = -\langle \nabla\Omega(\pi_c) - \nabla\Omega(\pi_a), \pi_c - \pi_b \rangle_{\mathcal{A}} + D_\Omega(\pi_b\|\pi_c) \quad (22)$$

Proof of Lemma 5. By Lemma 3, we have

$$D_\Omega(\pi_b\|\pi_a) - D_\Omega(\pi_c\|\pi_a) = -D_\Omega(\pi_c\|\pi_b) + \langle \nabla\Omega(\pi_a) - \nabla\Omega(\pi_b), \pi_c - \pi_b \rangle_{\mathcal{A}}.$$

We separate $\nabla\Omega(\pi_a) - \nabla\Omega(\pi_b)$ into $\nabla\Omega(\pi_a) - \nabla\Omega(\pi_c)$ and $\nabla\Omega(\pi_c) - \nabla\Omega(\pi_b)$ and write the rest of the derivation as follows.

$$\begin{aligned} & D_\Omega(\pi_b\|\pi_a) - D_\Omega(\pi_c\|\pi_a) \\ &= \underbrace{-D_\Omega(\pi_c\|\pi_b) + \langle \nabla\Omega(\pi_c) - \nabla\Omega(\pi_b), \pi_c - \pi_b \rangle_{\mathcal{A}}}_{\text{Eq. (21)}} + \langle \nabla\Omega(\pi_a) - \nabla\Omega(\pi_c), \pi_c - \pi_b \rangle_{\mathcal{A}} \\ &= D_\Omega(\pi_b\|\pi_c) + \langle \nabla\Omega(\pi_a) - \nabla\Omega(\pi_c), \pi_c - \pi_b \rangle_{\mathcal{A}} \end{aligned}$$

Therefore, we achieve the desired identity. \square

Combining above lemmas, we show a key argument to prove Theorem 1 in the following lemma.

Lemma 6. *Assume $\inf_{\pi \in \Pi} \mathbb{E}[f(\pi, \tau_t)] > 0$. Assume that Ω is ω -strongly convex and $\nabla\Omega$ is L -Lipschitz continuous for $\omega \geq 0$ and $L \geq 0$. If $\lim_{t \rightarrow \infty} \mathbb{E}_{\tau_{1:t}} [\sum_{i=0}^{\infty} \gamma^i D_\Omega(\pi_t(\cdot|s_i) \|\pi_E(\cdot|s_i))] = 0$ for $\pi_E \in \Pi$, then $\{\eta_t\}_{t=1}^{\infty}$ satisfies Eq. (9). Furthermore, if Ω is strongly smooth, then Theorem 1 (a) holds with some constants $n \in \mathbb{N}$ and $c > 0$.*

Proof of Lemma 6. First, we show the condition of $\lim_{t \rightarrow \infty} \eta_t = 0$. Assuming all states are decomposable¹, the condition $\lim_{t \rightarrow \infty} \mathbb{E}_{\tau_{1:t}} [\sum_{i=0}^{\infty} \gamma^i D_\Omega(\pi_t(\cdot|s_i) \|\pi_E(\cdot|s_i))] = 0$ implies $\lim_{t \rightarrow \infty} \mathbb{E}_{\tau_{1:t}} [\|\pi_t - \pi_E\|] = 0$, where $\|\cdot\|$ is the matrix norm induced by the p-norm on \mathcal{A} . Then, our aim is to show that the gradient of the strong convex function for π_t converges to $\nabla\Omega(\pi_E)$, i.e.

$$\lim_{t \rightarrow \infty} \mathbb{E}_{\tau_{1:t}} [\|\nabla\Omega(\pi_t) - \nabla\Omega(\pi_E)\|_*] = 0, \quad (23)$$

where $\|\cdot\|_*$ is the matrix norm induced by the q-norm and $\nabla\Omega(\pi)$ is a shorthand notation for $[\nabla\Omega(\pi_t^s)]_{s \in \mathcal{S}}$. To prove this argument, we use the continuity of $\nabla\Omega$ at π_E ; this means for any $\varepsilon > 0$, there exists some $0 < \delta \leq 1$ such that $\|\nabla\Omega(\pi) - \nabla\Omega(\pi_E)\|_* < \varepsilon$ whenever $\|\pi - \pi_E\| < \delta$.

¹The decomposability condition; Definition B.1 of Fu et al. [10]

When $\|\pi - \pi_E\| \geq \delta$, we apply the L -Lipschitz continuity assumption to find

$$\|\nabla\Omega(\pi) - \nabla\Omega(\pi_E)\|_* \leq L\|\pi - \pi_E\|, \quad (24)$$

where $\|\cdot\|_*$ is a matrix norm induced by the q -norm. Combining Eq. (23) and Eq. (24), we know that

$$\mathbb{E}_{\tau_{1:t}}[\|\nabla\Omega(\pi_t) - \nabla\Omega(\pi_E)\|_*] \leq \varepsilon + L \cdot \mathbb{E}_{\tau_{1:t}}[\|\pi_t - \pi_E\|]. \quad (25)$$

Since $\lim_{t \rightarrow \infty} \mathbb{E}_{\tau_{1:t}}[\|\pi_E - \pi_t\|] = 0$ ensures the existence of some $n \in \mathbb{N}$ such that for $t > n$, it holds that $\mathbb{E}_{\tau_{1:t}}[\|\pi_E - \pi_t\|] < \varepsilon/L$. Applying this inequality to Eq. (25), we have $\mathbb{E}_{\tau_{1:t}}[\|\nabla\Omega(\pi_t) - \nabla\Omega(\pi_E)\|_*] < 2\varepsilon$ for some $t > n$.

For temporal estimations, let us define the infimum of the expectation throughout the time as

$$\ell = \inf_{\pi \in \Delta_{\mathcal{A}}^{\mathcal{S}}} \mathbb{E}[\|\nabla\Omega(\pi_t) - \nabla\Omega(\bar{\pi}_{E,t})\|_*] > 0.$$

From Lemma 2, we have $\eta_t(\nabla\Omega(\pi_t^s) - \nabla\Omega(\bar{\pi}_{E,t}^s)) = \nabla\Omega(\pi_t^s) - \nabla\Omega(\pi_{t+1}^s)$ for every s . Taking the expectations, for every state s , the following inequality holds:

$$\eta_t \ell \leq \eta_t \mathbb{E}_{\tau_{1:t+1}}[\|\nabla\Omega(\pi_{t+1}^s) - \nabla\Omega(\bar{\pi}_{E,t}^s)\|_*] = \mathbb{E}_{\tau_{1:t+1}}[\|\nabla\Omega(\pi_t^s) - \nabla\Omega(\pi_{t+1}^s)\|_*] \quad \forall s \in \mathcal{S}.$$

Hence the convergence of the point $[\nabla\Omega(\pi_t^s)]_{s \in \mathcal{S}}$ is confirmed by taking the limit: $\lim_{t \rightarrow \infty} \eta_t = 0$.

Next, we show $\sum_{t=1}^{\infty} \eta_t = \infty$. By the ω -strong convexity by the L -Lipschitz continuity of Ω , we can find inequalities as

$$\langle \nabla\Omega(\pi^s) - \nabla\Omega(\tilde{\pi}^s), \pi^s - \tilde{\pi}^s \rangle_{\mathcal{A}} \leq L\|\pi^s - \tilde{\pi}^s\|^2 \leq \frac{2L}{\omega} D_{\Omega}(\pi^s \|\tilde{\pi}^s) \quad \forall s \in \mathcal{S}. \quad (26)$$

We note that $\|\pi_{t+1}^s - \bar{\pi}_{E,t+1}^s\| \leq \|\pi_t^s - \bar{\pi}_{E,t}^s\|$ so that there is a constant ε that satisfies $\mathbb{E}[\|\pi_{t+1}^s - \bar{\pi}_{E,t+1}^s\|] \geq \mathbb{E}[\|\pi_{t+1}^s - \bar{\pi}_{E,t}^s\|] + \varepsilon$. Therefore, taking expectations in Eq. (22) (and setting $\pi_a = \bar{\pi}_{E,t}^s$, $\pi_b = \pi_{t+1}^s$, and $\pi_c = \pi_t^s$) from Lemma 5, for the strongly convex Ω , we can find

$$\begin{aligned} \mathbb{E}_{\tau_{1:t+1}}[D_{\Omega}(\pi_{t+1}^s \|\bar{\pi}_{E,t+1}^s)] &\geq \mathbb{E}_{\tau_{1:t+1}}[D_{\Omega}(\pi_{t+1}^s \|\bar{\pi}_{E,t}^s)] + \varepsilon' \\ &\geq (1-a\eta_t) \mathbb{E}_{\tau_{1:t}}[D_{\Omega}(\pi_t^s \|\bar{\pi}_{E,t}^s)] + \mathbb{E}_{\tau_{1:t+1}}[D_{\Omega}(\pi_{t+1}^s \|\pi_t^s)] + \varepsilon' \\ &\geq (1-a\eta_t) \mathbb{E}_{\tau_{1:t}}[D_{\Omega}(\pi_t^s \|\bar{\pi}_{E,t}^s)] + \varepsilon'' \quad \forall s \in \mathcal{S}, \end{aligned} \quad \begin{aligned} & \text{Eq. (22)} \\ & \text{Eq. (27)} \end{aligned}$$

for some t and $0 < \varepsilon' < \varepsilon''$ when for $\lim_{t \rightarrow \infty} \eta_t = 0$. The positive constant $a := 2L/\omega$ is derived by the inequalities in Eq. (26).

Since $\lim_{t \rightarrow \infty} \eta_t = 0$, we can also find a constant $n \in \mathbb{N}$ such that $\eta_t \leq (3a)^{-1}$ for $t \geq n$. Applying the inequality $1 - x > \exp(-2x)$ for $x \in (0, 1/3]$, we derive another inequality

$$\mathbb{E}_{\tau_{1:t+1}}[D_{\Omega}(\pi_{t+1}^s \|\bar{\pi}_{E,t+1}^s)] \geq \exp(-2a\eta_t) \mathbb{E}_{\tau_{1:t}}[D_{\Omega}(\pi_t^s \|\bar{\pi}_{E,t}^s)], \quad \forall t \geq n \quad \forall s \in \mathcal{S}. \quad (28)$$

Applying this for $t = T-1, \dots, n$ yields

$$\begin{aligned} \mathbb{E}_{\tau_{1:T}}[D_{\Omega}(\pi_T^s \|\bar{\pi}_{E,T}^s)] &\geq \left(\prod_{t=n+1}^T \exp(-2a\eta_t) \right) \mathbb{E}_{\tau_{1:n}}[D_{\Omega}(\pi_n^s \|\bar{\pi}_{E,n}^s)] \\ &= \exp\left(-2a \cdot \sum_{t=n+1}^T \eta_t\right) \mathbb{E}_{\tau_{1:n}}[D_{\Omega}(\pi_n^s \|\bar{\pi}_{E,n}^s)]. \end{aligned} \quad (29)$$

Using Eq. (29), we conclude $\mathbb{E}_{\tau_{1:n}}[D_{\Omega}(\pi_n^s \|\bar{\pi}_{E,n}^s)] > 0$ for some s . Otherwise, we have that

$$\mathbb{E}_{\tau_{1:n}}[D_{\Omega}(\pi_n^s \|\bar{\pi}_{E,n}^s)] = \mathbb{E}_{\tau_{1:n+1}}[D_{\Omega}(\pi_{n+1}^s \|\bar{\pi}_{E,n+1}^s)] = 0 \quad \forall s \in \mathcal{S},$$

which leads to $\mathbb{E}_{\tau_{1:n}}[\|\pi_n - \bar{\pi}_{E,n}\|^2] = \mathbb{E}_{\tau_{1:n+1}}[\|\pi_{n+1} - \bar{\pi}_{E,n+1}\|^2] = 0$, according to Eq. (28). This implies $\pi_n = \bar{\pi}_{E,n} = \pi_{n+1}$ almost surely, leading to $\mathbb{E}[f(\pi_t, \tau_t)] = 0$. Essentially, this is a contradiction to the previous assumption $\inf_{\pi \in \Delta_{\mathcal{A}}^{\mathcal{S}}} \mathbb{E}[f(\pi, \tau_t)] > 0$; thus, $\mathbb{E}_{\tau_{1:n+1}}[D_{\Omega}(\pi_{n+1} \|\bar{\pi}_{E,n+1})] > 0$. Let us assume the ideal case in which the estimation process learns the exact π_E in $t \rightarrow \infty$. To satisfy the limit $\lim_{T \rightarrow \infty} \mathbb{E}_{\tau_{1:T}}[D_{\Omega}(\pi_T \|\bar{\pi}_{E,T})] = 0$ we see from Eq. (29) that $\sum_{t=1}^{\infty} \eta_t = \infty$.

Now, we show that Theorem 1 (a) holds. Since Ω is ω -strongly convex, so basically Ω^* is (ω^{-1}) -strongly smooth with respect to $\|\cdot\|_*$. On the other hand, the L -Lipschitz continuity of $\nabla\Omega$ implies L -strong smoothness of Ω ; thus, Ω^* is L -strongly convex.

Since $\lim_{t \rightarrow \infty} \|\nabla\Omega(\pi_t^s) - \nabla\Omega(\pi_{t+1}^s)\|_* = 0$ for $\forall t \geq n$ and $\forall s \in \mathcal{S}$, the condition $\eta_t \leq (3a)^{-1}$ induces

$$\begin{aligned} & \mathbb{E}_{\tau_{1:t+1}}[D_\Omega(\pi_{t+1}^s \|\bar{\pi}_{E,t+1}^s)] \\ & \geq (1-a\eta_t) \mathbb{E}_{\tau_{1:t}}[D(\pi_t^s \|\bar{\pi}_{E,t}^s)] + (2L)^{-1} \mathbb{E}_{\tau_{1:t+1}}[\|\nabla\Omega(\pi_t) - \nabla\Omega(\pi_{t+1})\|_*^2], \\ & \geq (1-a\eta_t) \mathbb{E}_{\tau_{1:t}}[D_\Omega(\pi_t^s \|\bar{\pi}_{E,t}^s)] + (2L)^{-1} \eta_t^2 \mathbb{E}_{\tau_{1:t+1}}[\|\nabla\Omega(\pi_t) - \nabla\Omega(\bar{\pi}_{E,t})\|_*]. \end{aligned} \quad \text{Lemma 2}$$

Using the Cauchy-Schwarz inequality, we obtain a lower bound of the last term as

$$\mathbb{E}_{\tau_{1:t}}[\|\nabla\Omega(\pi_t) - \nabla\Omega(\bar{\pi}_{E,t})\|_*^2] \geq \left\{ \mathbb{E}_{\tau_{1:t}}[\|\nabla\Omega(\pi_t) - \nabla\Omega(\bar{\pi}_{E,t})\|_*] \right\}^2 \geq \ell^2.$$

Thus, we obtain the final inequality for all $s \in \mathcal{S}$ as

$$\mathbb{E}_{\tau_{1:t+1}}[D_\Omega(\pi_{t+1}^s \|\bar{\pi}_{E,t+1}^s)] \geq (1-a\eta_t) \mathbb{E}_{\tau_{1:t}}[D_\Omega(\pi_t^s \|\bar{\pi}_{E,t}^s)] + (2L)^{-1}(\eta_t \ell)^2, \quad \forall t \geq n.$$

Applying this inequality from $t = T \geq n+1$ to $t = n+1$, we achieve

$$\begin{aligned} \mathbb{E}_{\tau_{1:T+1}}[D_\Omega(\pi_{T+1}^s \|\bar{\pi}_{E,T+1}^s)] & \geq \mathbb{E}_{\tau_{1:n}}[D_\Omega(\pi_n^s \|\bar{\pi}_{E,n}^s)] \prod_{t=n+1}^T (1-a\eta_t) \\ & \quad + (2L)^{-1} \ell^2 \sum_{t=n+1}^T \eta_t^2 \prod_{k=t+1}^T (1-a\eta_k) \\ & \geq (2L)^{-1} \ell^2 \sum_{t=n+1}^T \eta_t^2 \prod_{k=t+1}^T (1-a\eta_k). \end{aligned}$$

By the Cauchy-Schwarz inequality and our bound $0 < 1-a\eta_k \leq 1$ for $k \geq n$, we have

$$\sum_{t=n+1}^T \eta_t \prod_{k=t+1}^T (1-a\eta_k) \leq \left\{ \sum_{t=n+1}^T \eta_t^2 \prod_{k=t+1}^T (1-a\eta_k) \right\}^{1/2} (T-n)^{1/2}.$$

Hence

$$\begin{aligned} \sum_{t=n+1}^T \eta_t^2 \prod_{k=t+1}^T (1-a\eta_k) & \geq \frac{1}{a^2(T-n)} \left(\sum_{t=n+1}^T a\eta_t \prod_{k=t+1}^T (1-a\eta_k) \right)^2 \\ & = \frac{1}{a^2(T-n)} \left(\sum_{t=n+1}^T (1 - (1-a\eta_t)) \prod_{k=t+1}^T (1-a\eta_k) \right)^2 \\ & = \frac{1}{a^2(T-n)} \left(\sum_{t=n+1}^T \left[\prod_{k=t+1}^T (1-a\eta_k) - \prod_{k=t}^T (1-a\eta_k) \right] \right)^2 \\ & \geq \frac{1}{a^2(T-n)} \left(\sum_{t=n+1}^T 1 - \prod_{k=t}^T (1-a\eta_k) \right)^2 \\ & \geq \frac{1}{a^2(T-n)} (1 - (1-a\eta_{n+1}))^2 = \frac{\eta_{n+1}^2}{T-n} \end{aligned}$$

Therefore, we obtain the lower bound of

$$\mathbb{E}_{\tau_{1:T}}[D_\Omega(\pi_{T+1} \|\bar{\pi}_{E,T+1})] \geq \frac{\eta_{n+1}^2 (2L)^{-1} \ell^2}{T-n}.$$

Since the Bregman divergence is assumed to be bounded for all states, the sequence $\{\gamma^i D_\Omega(\pi_t^{s_i} \|\pi_t^{s_i})\}$ will converge as $i \rightarrow \infty$. Applying the monotone convergence theorem, we can interchange expectation and summation, which yields

$$\begin{aligned} \mathbb{E}_{\tau_{1:T}} \left[\sum_{i=0}^{\infty} \gamma^i D_\Omega(\pi_T(\cdot|s_i) \|\bar{\pi}_{E,T}(\cdot|s_i)) \right] &= \sum_{i=0}^{\infty} \mathbb{E}_{\tau_{1:T}} \left[\gamma^i D_\Omega(\pi_T(\cdot|s_i) \|\bar{\pi}_{E,T}(\cdot|s_i)) \right] \\ &= \sum_{i=0}^{\infty} \gamma^i \mathbb{E}_{\tau_{1:T}} \left[D_\Omega(\pi_T(\cdot|s_i) \|\bar{\pi}_{E,T}(\cdot|s_i)) \right] \\ &\geq \frac{\eta_{n+1}^2 (2L - 2L\gamma)^{-1} \ell^2}{T - n}, \quad \forall T \geq n. \end{aligned}$$

This verifies Theorem 1 (a) with the constant $c = \eta_{n+1}^2 (2L - 2L\gamma)^{-1} \ell^2$. \square

Lastly, we show convergence to a unique fixed point of π_* using the particular form of η_t in Eq. (9).

Lemma 7. *If $\{\eta_t\}_{t=1}^{\infty}$ satisfies Eq. (9), $\lim_{t \rightarrow \infty} \mathbb{E}_{\tau_{1:t}} [\sum_{i=0}^{\infty} \gamma^i D_\Omega(\pi_*^s \|\pi_t^s)] = 0$. Furthermore, if the step size takes the form $\eta_t = \frac{4}{t+1}$, then $\mathbb{E}_{\tau_{1:T}} [\sum_{i=0}^{\infty} \gamma^i D_\Omega(\pi_*^s \|\pi_T^s)] = \mathcal{O}(1/T)$.*

Proof of Lemma 7. According to Lemma 4 and the fundamental identity of Bregman divergence for the convex conjugate Ω^* , the one-step progress regarding $\bar{\pi}_{E,t}^s$ can be written as

$$\begin{aligned} D_\Omega(\pi_*^s \|\pi_{t+1}^s) - D_\Omega(\pi_*^s \|\pi_t^s) &= \langle \nabla \Omega(\pi_t^s) - \nabla \Omega(\pi_{t+1}^s), \pi_*^s - \pi_t^s \rangle_A + D_\Omega(\pi_t^s \|\pi_{t+1}^s) \\ &= \eta_t \langle \nabla \Omega(\pi_t^s) - \nabla \Omega(\bar{\pi}_{E,t}^s), \pi_*^s - \pi_t^s \rangle_A + D_{\Omega^*}(\nabla \Omega(\pi_{t+1}^s) \|\nabla \Omega(\pi_t^s)), \end{aligned} \quad (30)$$

for all $s \in \mathcal{S}$. As ω -strong convexity of Ω implies the (ω^{-1}) -strong smoothness of Ω^* , we have

$$D_{\Omega^*}(\nabla \Omega(\pi_{t+1}^s) \|\nabla \Omega(\pi_t^s)) \leq \frac{1}{2\omega} \|\nabla \Omega(\pi_{t+1}^s) - \nabla \Omega(\pi_t^s)\|_*^2 = \frac{\eta_t^2}{2\omega} \|\nabla \Omega(\bar{\pi}_{E,t}^s) - \nabla \Omega(\pi_t^s)\|_*^2 \quad (31)$$

Then, we bound $\|\nabla \Omega(\bar{\pi}_{E,t}^s) - \nabla \Omega(\pi_t^s)\|_*^2$ by $2\|\nabla \Omega(\pi_t^s) - \nabla \Omega(\pi_*^s)\|_*^2 + 2\|\nabla \Omega(\pi_*^s) - \nabla \Omega(\bar{\pi}_{E,t}^s)\|_*^2$, following the work of Lei and Zhou [17]. Since $\nabla \Omega$ is cocoercive with $\frac{1}{L}$ by the Lipschitz continuity of $\nabla \Omega$, we obtain

$$\|\nabla \Omega(\pi_t^s) - \nabla \Omega(\pi_*^s)\|_*^2 \leq L \langle \nabla \Omega(\pi_*^s) - \nabla \Omega(\pi_t^s), \pi_*^s - \pi_t^s \rangle$$

thus, using Eq. (30), we get

$$\begin{aligned} D_\Omega(\pi_*^s \|\pi_{t+1}^s) - D_\Omega(\pi_*^s \|\pi_t^s) &\leq \eta_t \langle \nabla \Omega(\pi_*^s) - \nabla \Omega(\bar{\pi}_{E,t}^s), \pi_*^s - \pi_t^s \rangle \\ &\quad - \left(1 - \frac{\eta_t L}{\omega}\right) \eta_t \langle \nabla \Omega(\pi_*^s) - \nabla \Omega(\pi_t^s), \pi_*^s - \pi_t^s \rangle + \frac{\eta_t^2}{\omega} (\|\nabla \Omega(\pi_*^s) - \nabla \Omega(\bar{\pi}_{E,t}^s)\|_*^2). \end{aligned} \quad (32)$$

By taking expectation, it follows that there exists $n \in \mathbb{N}$ such that $\eta_t \leq \frac{\omega}{2L}$ for $t \geq n$ holds

$$\begin{aligned} \mathbb{E}_{\tau_{1:t+1}} [D_\Omega(\pi_*^s \|\pi_{t+1}^s)] &\leq \mathbb{E}_{\tau_{1:t}} \left[D_\Omega(\pi_*^s \|\pi_t^s) - \frac{\eta_t}{2} D_\Omega(\pi_*^s \|\pi_t^s) + \frac{\eta_t^2}{\omega} \|\nabla \Omega(\pi_*^s) - \nabla \Omega(\bar{\pi}_{E,t}^s)\|_*^2 \right], \\ &\leq \mathbb{E}_{\tau_{1:t}} \left[D_\Omega(\pi_*^s \|\pi_t^s) - \frac{\eta_t}{2} D_\Omega(\pi_*^s \|\pi_t^s) \right] + z\eta_t^2, \end{aligned} \quad (33)$$

where z is the constant $z = \frac{1}{\omega} \mathbb{E}[\|\nabla \Omega(\pi_*) - \nabla \Omega(\bar{\pi}_{E,t}^s)\|_*^2]$. Let $\{A_t\}_{t=1}^{\infty}$ denote a sequence of $A_t = \sup_{s \in \mathcal{S}} \mathbb{E}_{\tau_{1:t}} [D_\Omega(\pi_*^s \|\pi_t^s)]$. Then we have

$$A_{t+1} \leq \left(1 - \frac{\eta_t}{2}\right) A_t + z\eta_t^2, \quad \forall t \geq n. \quad (34)$$

For a constant $h > 0$, we claim that $A_{t_1} < h$ for some $t_1 > n'$. Assume that this is not true, and we find some $t_2 \geq t_1$ such that $A_t > h$, $\forall t \geq t_2$. Since $\lim_{t \rightarrow \infty} \eta_t = 0$, there are some $t > t_3 > t_2$ that $\eta_t \leq \frac{h}{4b}$. However, Eq. (34) tells us that for $t \geq t_3$,

$$A_{t+1} \leq \left(1 - \frac{\eta_t}{2}\right) A_t + z\eta_t^2 \leq A_{t_3} - \frac{h}{4} \sum_{k=t_3}^t \eta_k \rightarrow -\infty \quad (\text{as } t \rightarrow \infty).$$

This is a contradiction, which verifies $A_t < h$ for $t > n'$. Since $\lim_{t \rightarrow \infty} \eta_t = 0$, we can find some η_t that makes A_t monotonically decreasing. Then, we can conclude that the nonnegative sequence $\{A_t\}_{t=1}^{\infty}$ converges by iteratively applying the upper bounds.

We now prove Theorem 1 (b) under the consideration of the condition $\eta_t = \frac{4}{t+1}$. The estimate becomes

$$A_{t+1} \leq \left(1 - \frac{2}{t+1}\right)A_t + \frac{16z}{(t+1)^2}, \quad \forall t \geq n.$$

It follows the recurrence relation is

$$t(t+1)A_{t+1} \leq (t-1)tA_t + 16z, \quad \forall t \geq n.$$

Iteratively applying this relation, we obtain the general form of inequality.

$$(T-1)TA_T \leq (n-1)nA_n + 16z(T-n), \quad \forall T \geq n,$$

therefore we obtain the inequality as follows:

$$\mathbb{E}_{\tau_{1:T}}[D_{\Omega}(\pi_*^s \| \pi_T^s)] \leq \frac{(n-1)n\mathbb{E}_{\tau_{1:n}}[D_{\Omega}(\pi_*^s \| \pi_n^s)]}{(T-1)T} + \frac{16z}{T}, \quad \forall T \geq n, \quad \forall s \in \mathcal{S}.$$

By applying the monotone convergence theorem, we can interchange expectation and summation, which yields similar result to formultion from Proof of Lemma 6

$$\mathbb{E}_{\tau_{1:T}}\left[\sum_{i=1}^{\infty} \gamma^i D_{\Omega}(\pi_*(\cdot | s_i) \| \pi_T(\cdot | s_i))\right] = \mathcal{O}\left(\frac{1}{T}\right).$$

Therefore, the proof is complete. \square

A.3 Proof of Theorem 2

Necessity. First, we rewrite the inequality in Eq. (27) as

$$\mathbb{E}_{\tau_{1:t+1}}[D_{\Omega}(\pi_{t+1}^s \| \bar{\pi}_{E,t+1}^s)] \geq (1 - 2L\omega^{-1}\eta_t) \mathbb{E}_{\tau_{1:t}}[D_{\Omega}(\pi_t^s \| \bar{\pi}_{E,t}^s)], \quad \forall s \in \mathcal{S}. \quad (35)$$

Since we assume that η_t converges to 0 from previous arguments, consider the step size sequence $0 < \eta_t \leq \frac{\omega}{(2+\kappa)L}$ for $\kappa > 0$ and $t \geq n$ where $\forall n \in \mathbb{N}$. Denote a constant $\tilde{a} = \frac{2+\kappa}{2} \log \frac{2+\kappa}{\kappa}$ and apply the elementary inequality

$$1 - x \geq \exp(-\tilde{a}x), \quad \text{such that } 0 < x \leq \frac{2}{2+\kappa}$$

From Eq. (35), it can be obtained that

$$\mathbb{E}_{\tau_{1:t+1}}[D_{\Omega}(\pi_{t+1}^s \| \bar{\pi}_{E,t+1}^s)] \geq \exp(-2\tilde{a}L\omega^{-1}\eta_t) \mathbb{E}_{\tau_{1:t}}[D_{\Omega}(\pi_t^s \| \bar{\pi}_{E,t}^s)].$$

Applying this inequality iteratively for $t = n, \dots, T-1$ gives

$$\begin{aligned} \mathbb{E}_{\tau_{1:T}}[D_{\Omega}(\pi_T^s \| \bar{\pi}_{E,T}^s)] &\geq \mathbb{E}_{\tau_{1:n}}[D_{\Omega}(\pi_n^s \| \bar{\pi}_{E,n}^s)] \prod_{t=n}^{T-1} \exp(-2\tilde{a}L\omega^{-1}\eta_t) \\ &= \exp\left\{-2\tilde{a}L\omega^{-1} \sum_{t=n}^{T-1} \eta_t\right\} \mathbb{E}_{\tau_{1:n}}[D_{\Omega}(\pi_n^s \| \bar{\pi}_{E,n}^s)] \quad \forall s \in \mathcal{S}. \end{aligned} \quad (36)$$

From the assumption $\pi_E \neq \pi_n$, we have $D_{\Omega}(\pi_n^s \| \bar{\pi}_{E,n}^s) > 0$ for some states. Therefore, by Eq. (36), the convergence $\lim_{t \rightarrow \infty} \mathbb{E}_{\tau_{1:t}}[D_{\Omega}(\pi_t^s \| \bar{\pi}_{E,t}^s)] = 0$ for all states implies $\sum_{t=1}^{\infty} \eta_t = \infty$.

Sufficiency. We use Eq. (34) in the proof of Lemma 7. In the optimal case, $\|\nabla \Omega(\pi_*) - \Omega(\bar{\pi}_{E,t})\|_* = 0$, so (34) takes the form (we can choose $n = 1$ by Eq. (33))

$$A_{t+1} \leq \frac{\eta_t}{2} A_t, \quad \forall t \in \mathbb{N}, \quad (37)$$

where $A_t = \sup_{s \in \mathcal{S}} \mathbb{E}_{\tau_{1:t}} [D_\Omega(\pi_*^s \| \pi_t^s)]$ (and also $A_t = \sup_{s \in \mathcal{S}} \mathbb{E}_{\tau_{1:t}} [D_\Omega(\pi_E^s \| \pi_t^s)]$ for the specific parameterization of $\pi_E \in \Pi$). Therefore, for any $0 < h < 1$, there must exist some $t_1 \in \mathbb{N}$ such that $A_t \leq h$ for $t \geq t_1$. Otherwise, $A_t > h$ for every $t \geq t_2$ with $t_2 \geq t_1$, which leads to a contradiction:

$$A_{t+1} \leq A_{t_2} - \frac{h}{2} \sum_{k=t_1}^t \eta_k \rightarrow -\infty \text{ (as } t \rightarrow \infty\text{).}$$

Eq. (37) also tells us that the sequence $\{A_t\}_{t=1}^\infty$ is monotonically decreasing. Hence $A_t \leq h$ for every $t \geq t_1$, which proves the convergence with respect to the least upper bound of Bregman divergences by combining with Eq. (37)

$$\lim_{t \rightarrow \infty} \sup_{s \in \mathcal{S}} \mathbb{E}_{\tau_{1:t}} [D_\Omega(\pi_*^s \| \pi_t^s)] = \lim_{t \rightarrow \infty} A_t = 0.$$

We now prove the second point in Theorem 2 which is under the special condition of $\eta_t \equiv \eta_1$. It follows from Eq. (35) that $A_T \geq (1 - 2L\omega^{-1}\eta_1)^{T-1} A_1$. Hence, Eq (37) translates to

$$A_{t+1} \leq (1 - \eta_1/2) A_t,$$

from which we find $A_T \leq (1 - \eta_1/2)^{T-1} A_1$ by iteration starting from $t = 1$. Therefore, the second point is verified the theorem with $c_1 = 1 - \frac{2L\eta_1}{\omega}$ and $c_2 = 1 - \frac{\eta_1}{2}$. \square

A.4 Proof of Proposition 1

The proof of Proposition 1 is based on the Doob's forward convergence theorem.

Theorem 3 (Doob's forward convergence theorem). *Let $\{X_t\}_{t \in \mathbb{N}}$ be a sequence of nonnegative random variables and let $\{\mathcal{F}_t\}_{t \in \mathbb{N}}$ be a filtration with $\mathcal{F}_t \subset \mathcal{F}_{t+1}$ for every $t \in \mathbb{N}$. Assume that $\mathbb{E}[X_{t+1} | \mathcal{F}_t] \leq X_t$ almost surely for every $t \in \mathbb{N}$. Then the sequence $\{X_t\}$ converges to a nonnegative random variable X_∞ almost surely.*

We follow the proof of Lemma 7 and apply Eq. (32). Since $\langle \pi_*^s - \pi_t^s, \nabla \Omega(\pi_*^s) - \nabla \Omega(\pi_t^s) \rangle \geq 0$ for all $s \in \mathcal{S}$, Eq. (32) implies: there exists $n \in \mathbb{N}$ that

$$\mathbb{E}_{\tau_t} [D_\Omega(\pi_*^s \| \pi_{t+1}^s)] \leq D_\Omega(\pi_*^s \| \pi_t^s) + \frac{\eta_t^2}{\omega} \mathbb{E} [\|\nabla \Omega(\pi_*) - \nabla \Omega(\bar{\pi}_{E,t})\|_*^2], \quad \forall t \geq n, \forall s \in \mathcal{S}, \quad (38)$$

and since the step size is scheduled as $\lim_{t \rightarrow \infty} \eta_t = 0$, the following equation also holds:

$$\mathbb{E}_{\tau_t} \left[\sup_{s \in \mathcal{S}} D_\Omega(\pi_*^s \| \pi_{t+1}^s) \right] \leq \sup_{s \in \mathcal{S}} D_\Omega(\pi_*^s \| \pi_t^s) + \frac{\eta_t^2}{\omega} \mathbb{E} [\|\nabla \Omega(\pi_*) - \nabla \Omega(\bar{\pi}_{E,t})\|_*^2], \quad \forall t \geq n', \quad (39)$$

for some $n' \in \mathbb{N}$. Then, the condition $\sum_{t=1}^\infty \eta_t^2 < \infty$ enables us to define a stochastic process $\{X_t\}$:

$$X_t := \sup_{s \in \mathcal{S}} D_\Omega(\pi_*^s \| \pi_{t+1}^s) + \frac{1}{\omega} \mathbb{E} [\|\nabla \Omega(\pi_*) - \nabla \Omega(\bar{\pi}_{E,t})\|_*^2] \sum_{i=t+1}^\infty \eta_i^2.$$

Thus, by Eq. (39), it is straightforwardly derived that there exists $n \in \mathbb{N}$ that $\mathbb{E}_{\tau_t} [X_{t+1}] \leq X_t$ for $t \geq n$. Since $X_t \geq 0$, the stochastic process $\{X_t\}_{t=n+1}^\infty$ is a submartingale (equivalently, $\{-X_t\}_{t=n+1}^\infty$ is a supermartingale). By Theorem 3, the sequence $\{X_t\}_{t \geq 1}$ converges to a nonnegative random variable X_∞ almost surely. Therefore, $D_\Omega(\pi_*^s \| \pi_t^s)$ converges for every state.

According to Fatou's lemma, and using the convergence of $\lim_t \mathbb{E}_{\tau_{1:t}} [\sum_{i=0}^\infty \gamma^i D_\Omega(\pi_*^s \| \pi_t^s)] = 0$ proved by Lemma 7, we obtain

$$\mathbb{E} \left[\lim_{t \rightarrow \infty} \sum_{i=0}^\infty \gamma^i D_\Omega(\pi_*(\cdot | s_i) \| \pi_t(\cdot | s_i)) \right] \leq (1-\gamma)^{-1} \liminf_{t \rightarrow \infty} \mathbb{E}_{\tau_{1:t}} \left[\sum_{i=0}^\infty \gamma^i D_\Omega(\pi_*^s \| \pi_t^s) \right] = 0.$$

Therefore, it can be concluded that the sequence of costs $\left\{ \sum_{i=0}^\infty \gamma^i D_\Omega(\pi_*(\cdot | s_i) \| \pi_t(\cdot | s_i)) \right\}_{t \in \mathbb{N}}$ converges to 0 almost surely. \square

B Tsallis Entropy and Associated Bregman Divergence Among Full Covariance Multivariate Gaussian Distributions

This appendix **reintroduces** derivations of Bregman divergences and regularized reward functions for tractable computation when Ω is the Tsallis entropy regularizer, which were previously proposed by Nielsen and Nock [53] and Jeon et al. [18]. And then, we delineate a distinct parameterization used in this paper for modeling Gaussian distribution policies equipped with full covariance matrices.

The standard form of the exponential family is represented as

$$\exp\{\langle\theta, t(x)\rangle - F(\theta) + k(x)\}. \quad (40)$$

The generalized parameterization of the multi-variate Gaussian is defined as follows:

$$\begin{aligned} \theta &= \begin{bmatrix} \Sigma^{-1}\mu \\ -\frac{1}{2}\Sigma^{-1} \end{bmatrix} = \begin{bmatrix} \theta_1 \\ \theta_2 \end{bmatrix}, \\ t(x) &= \begin{bmatrix} x \\ xx^\top \end{bmatrix}, \\ F(\theta) &= -\frac{1}{4}\theta_1^\top\theta_2^{-1}\theta_1 + \frac{1}{2}\ln|-\pi\theta_2^{-1}| = \frac{1}{2}\mu^\top\Sigma^{-1}\mu + \frac{1}{2}\ln(2\pi)^d|\Sigma|, \\ k(x) &= 0, \end{aligned}$$

where we can analytically recover the Gaussian distribution [53]

$$\begin{aligned} &\exp\{\langle\theta, t(x)\rangle - F(\theta) + k(x)\} \\ &= \exp\left\{\mu^\top\Sigma^{-1}x - \frac{1}{2}\text{tr}(\Sigma^{-1}xx^\top) - \frac{1}{2}\mu^\top\Sigma^{-1}\mu + \frac{1}{2}\ln(2\pi)^d|\Sigma|\right\} \\ &= \frac{1}{(2\pi)^{d/2}|\Sigma|^{1/2}} \exp\left\{\mu^\top\Sigma^{-1}x - \frac{1}{2}x^\top\Sigma^{-1}x - \frac{1}{2}\mu^\top\Sigma^{-1}\mu\right\} \\ &= \frac{1}{(2\pi)^{d/2}|\Sigma|^{1/2}} \exp\left\{\frac{1}{2}(x - \mu)^\top\Sigma^{-1}(x - \mu)\right\}. \end{aligned} \quad (41)$$

For two distributions π and $\hat{\pi}$ with $k(x) = 0$, Nielsen and Nock [53] proposed the function $I(\cdot)$:

$$I(\pi, \hat{\pi}; \alpha, \beta) = \int \pi(x)^\alpha \hat{\pi}(x)^\beta dx = \exp\{F(\alpha\theta + \beta\hat{\theta}) - \alpha F(\theta) - \beta F(\hat{\theta})\}$$

where the detailed derivation is as follows:

$$\begin{aligned} &\int \pi(x)^\alpha \hat{\pi}(x)^\beta dx \\ &= \int \exp\{\alpha\langle\theta, t(x)\rangle - \alpha F(\theta) + \beta\langle\hat{\theta}, t(x)\rangle - \beta F(\hat{\theta})\} dx \\ &= \int \exp\{\langle\alpha\theta + \beta\hat{\theta}, t(x)\rangle - F(\alpha\theta + \beta\hat{\theta})\} \exp\{F(\alpha\theta + \beta\hat{\theta}) - \alpha F(\theta) - \beta F(\hat{\theta})\} dx \\ &= \exp\{F(\alpha\theta + \beta\hat{\theta}) - \alpha F(\theta) - \beta F(\hat{\theta})\} \int \exp\{\langle\alpha\theta + \beta\hat{\theta}, t(x)\rangle - F(\alpha\theta + \beta\hat{\theta})\} dx \\ &= \exp\{F(\alpha\theta + \beta\hat{\theta}) - \alpha F(\theta) - \beta F(\hat{\theta})\}. \end{aligned}$$

B.1 Tsallis entropy of full covariance Gaussian distributions

For $\varphi(x; q) = \frac{1}{q-1}(x^{q-1} - 1)$, the Tsallis entropy can be written as

$$\begin{aligned} \mathcal{T}_q(\pi) &:= -\mathbb{E}_{x \sim \pi} \varphi(x; q) = \int \pi(x) \frac{1 - \pi(x)^{q-1}}{q-1} dx \\ &= \frac{1 - \int \pi(x)^q dx}{q-1} = \frac{1}{q-1}(1 - I(\pi, \pi; q, 0)) \\ &= \frac{1 - \exp(F(q\theta) - qF(\theta))}{q-1}. \end{aligned}$$

If π is a multivariate Gaussian distribution, we have

$$F(q\theta) = \frac{q}{2}\mu^\top \Sigma^{-1}\mu + \frac{1}{2}\ln(2\pi)^d|\Sigma| - \frac{1}{2}\ln q^d.$$

Since a covariance matrix is a symmetric positive semi-definite matrix, the LDL decomposition (a variant of Cholesky decomposition) can be applied, which separates the covariance matrix into $\Sigma = L \text{diag}\{\sigma_1^2, \dots, \sigma_d^2\} L^\top$ where L denotes a unit lower triangular matrix and $\text{diag}\{\sigma_1^2, \dots, \sigma_d^2\}$ denotes a diagonal matrix with positive entries. Then we have

$$\begin{aligned} F(q\theta) - qF(\theta) &= (1-q)\left\{\frac{d}{2}\ln 2\pi + \frac{1}{2}\ln|\Sigma| - \frac{d\ln q}{2(1-q)}\right\} \\ &= (1-q)\left\{\frac{d}{2}\ln 2\pi + \frac{1}{2}\ln \prod_{i=1}^d \sigma_i^2 - \frac{d\ln q}{2(1-q)}\right\} \\ &= (1-q)\sum_{i=1}^d \left\{\frac{\ln 2\pi}{2} + \ln \sigma_i - \frac{\ln q}{2(1-q)}\right\}. \end{aligned}$$

B.2 Tractable Form of ψ_π

For separable Ω , ψ_π is written as [18]

$$\psi_\pi(s, a) = -f'(s, a) + \mathbb{E}_{a \sim \pi}[f'(\pi(a|s)) - \varphi(a|s)]$$

where $\varphi(x) = \frac{k}{q-1}(1-x^{q-1})$ and accordingly $f(x) = x\varphi(x)$. For the gradient of $f(\cdot)$, we have

$$\begin{aligned} f'(x) &= \frac{k}{q-1}(1-qx^{q-1}) \\ &= \frac{k}{q-1}(q-qx^{q-1}-(q-1)) \\ &= \frac{qk}{q-1}(1-x^{q-1}) - k \\ &= q\varphi(x) - k. \end{aligned}$$

Taking the expectation yields Tsallis entropy as follows.

$$\mathbb{E}_{x \sim \pi}[-f'(x; \pi) + \varphi(x)] = \mathbb{E}_{x \sim \pi}[k - q\varphi(x) + \varphi(x)] = (1-q)\mathcal{T}_q^k(\pi) + k.$$

For a multivariate Gaussian distribution π , the tractable form of $\mathbb{E}_{x \sim \pi}[-f'(x) + \varphi(x)]$ can be derived by using that of Tsallis entropy $\mathcal{T}_q^k(\pi)$ of π . Thus ψ_π can be rewritten as

$$\psi_\pi(s, a) = q\varphi(s) + (q-1)\mathcal{T}_q^k(\pi)$$

In the special case of $q = 1$ and $k = 1$, we have $\psi_\pi(s, a) = \log \pi(a|s)$.

B.3 Bregman Divergence with Tsallis Entropy Regularization

We consider the following form of the Bregman divergence:

$$\int \pi(x) \left\{ f'(\hat{\pi}(x)) - \omega(\pi(x)) \right\} dx - \int \hat{\pi}(x) \left\{ f'(\hat{\pi}(x)) - \omega(\hat{\pi}(x)) \right\} dx$$

For $\omega(x) = \frac{k}{q-1}(1-x^{q-1})$, $f'(x) = \frac{k}{q-1}(1-qx^{q-1}) = q\varphi(x) - k$, and $k = 1$, the above form is equal to

$$\begin{aligned} &\int \pi(x) \left[\frac{1-q\hat{\pi}(x)^{q-1}}{q-1} \right] dx - \mathcal{T}_q(\pi) - (q-1)\mathcal{T}_q(\hat{\pi}) + 1 \\ &= \frac{1}{q-1} - \frac{q}{q-1} \int \pi(x) \hat{\pi}(x)^{q-1} dx - \mathcal{T}_q(\pi) - (q-1)\mathcal{T}_q(\hat{\pi}) + 1 \\ &= \frac{q}{q-1} - \frac{q}{q-1} \int \pi(x) \hat{\pi}(x)^{q-1} dx - \mathcal{T}_q(\pi) - (q-1)\mathcal{T}_q(\hat{\pi}). \end{aligned}$$

Let us define two multivariate Gaussian distributions as follows:

$$\pi(x) = \mathcal{N}(x; \mu, \Sigma), \mu = [\mu_1, \dots, \mu_d]^\top, \Sigma = L \text{diag}(\sigma_1^2, \dots, \sigma_d^2) L^\top,$$

$$\hat{\pi}(x) = \mathcal{N}(x; \hat{\mu}, \hat{\Sigma}), \hat{\mu} = [\hat{\mu}_1, \dots, \hat{\mu}_d]^\top, \hat{\Sigma} = \hat{L} \text{diag}(\hat{\sigma}_1^2, \dots, \hat{\sigma}_d^2) \hat{L}^\top,$$

where L and \hat{L} denote unit lower triangular matrices. We have

$$\int \pi(x) \hat{\pi}(x)^{q-1} dx = I(\pi, \hat{\pi}; 1, q-1) = \exp \{F(\theta') - F(\theta) - (q-1)F(\hat{\theta})\},$$

where

$$\theta = \begin{bmatrix} \Sigma^{-1}\mu \\ -\frac{1}{2}\Sigma^{-1} \end{bmatrix}$$

$$\hat{\theta} = \begin{bmatrix} \hat{\Sigma}^{-1}\mu \\ -\frac{1}{2}\hat{\Sigma}^{-1} \end{bmatrix}$$

$$\theta' = \theta + (q-1)\hat{\theta} = \begin{bmatrix} \Sigma^{-1}\mu + (q-1)\hat{\Sigma}^{-1}\mu \\ -\frac{1}{2}(\Sigma^{-1} + (q-1)\hat{\Sigma}^{-1}) \end{bmatrix} = \begin{bmatrix} \theta'_1 \\ \theta'_2 \end{bmatrix}$$

and

$$F(\theta) = \frac{1}{2}\mu^\top \Sigma^{-1}\mu + \frac{1}{2}\ln(2\pi)^d |\Sigma| = \frac{1}{2}(\mu)^\top \Sigma^{-1}\mu + \sum_{i=1}^d \frac{\ln 2\pi}{2} + \ln \sigma_i,$$

$$F(\hat{\theta}) = \frac{1}{2}\hat{\mu}^\top \hat{\Sigma}^{-1}\hat{\mu} + \frac{1}{2}\ln(2\pi)^d |\hat{\Sigma}| = \frac{1}{2}(\hat{\mu})^\top \hat{\Sigma}^{-1}\hat{\mu} + \sum_{i=1}^d \frac{\ln 2\pi}{2} + \ln \hat{\sigma}_i,$$

$$F(\theta + (q-1)\hat{\theta}) = -\frac{1}{4}(\theta'_1)^\top (\theta'_2)^{-1}(\theta'_1) + \frac{1}{2}\ln|\pi(\theta'_2)^{-1}|$$

B.4 Parameterization of the full covariance matrix using the LDL decomposition

Computing the Bregman divergence for multi-variate Gaussian distributions is challenging since the derivations involve inverses, determinants, and multiplications regarding Σ . Previous approaches did not address this issue and typically enforced Σ to be a diagonal matrix with positive entries. Motivated by Pourahmadi [54], we propose to mitigate the computations regarding a covariance matrix using the LDL decomposition $\Sigma = L \text{diag}\{\sigma_1^2, \dots, \sigma_d^2\} L^\top$ at the parameterization level. It enables us to implement relatively simple and numerically safe computations such as

$$\Sigma^{-1} = L^{-1} \text{diag}(1/\sigma)(L^{-1})^\top, \quad (42)$$

$$|\Sigma| = \sum_{i=1}^d \ln \sigma_i. \quad (43)$$

where L is a unit lower triangular matrix. Finding an inverse matrix of a unit triangular matrix can be computed by $\mathcal{O}(d^2)$ where the output is always a unit triangular matrix. Using the positive definiteness of Σ , the parameterization based on LDL decomposition allows a number of efficient computations for dealing with covariance matrices in practice while preserving the symmetry and the positive semi-definite matrix of Σ on the parameterization level. We utilized these findings on implementing the full covariance Gaussian policies and regularized reward functions.

C Implementation Details

C.1 Normalizing IRL rewards

Unnormalized rewards of the IRL algorithm often mislead the agent to take unnecessary awareness of *termination* in finite-horizon MDPs [12]. For this point, IRL algorithms need to remove the difference between regarding steps depending on the MDP's time. Doob's optimal stopping theorem formally states that the expected value of a martingale at a stopping time is equal to its initial expectation. Assume a martingale makes the entire procedure a fair game on average, which means nothing can be gained by stopping the play.

Theorem 4 (Doob’s optimal stopping theorem). *Let a process $\{X_t\}_{t=1}^\infty$ be a martingale and τ be a stopping time with respect to filtration $\{\mathcal{F}_t\}_{t \geq 1}$. Assume that one of the conditions holds:*

- (a) τ is almost surely bounded, i.e., there exists a constant $c \in \mathbb{N}$ such that $\tau \leq c$.
- (b) τ has finite expectation and the conditional expectations of the absolute value of the martingale increments almost surely bounded, more precisely, $\mathbb{E}[\tau] < \infty$ and there exists a constant c such that $\mathbb{E}[|X_{t+1} - X_t| \mid \mathcal{F}_t] \leq c$ almost surely on the event $\{\tau > t\}$ for all $t \geq 0$.
- (c) There exists a constant c such that $|X_{\min\{t, \tau\}}| \leq c$ almost surely for all $t \geq 0$. Then X_τ is an almost surely well-defined random variable and $\mathbb{E}[X_\tau] = \mathbb{E}[X_0]$.

Then X_∞ is integrable and $\mathbb{E}[X_\infty] = \mathbb{E}[X_0]$

Doob’s optimal stopping theorem states one of the necessary conditions of IRL reward of normalizing the reward measures and making them a martingale even for finite-horizon benchmarks. In addition to the analyses of [10, 18] regarding reward shaping and normalization, mean-zero rewards for training agents have the additional property of preventing the termination awareness, as stated by the optimal stopping theorem. Therefore, we suggest normalizing with the moving mean of intermediate values of regularized rewards and updating the RL algorithm with mean-subtracted rewards.

C.2 Transformation between π_ϕ and ψ_ϕ

In general, the regularized reward operation $\Psi_\Omega(\Pi)$ (as well as the Bregman divergence) is intractable to be computed. However, some tractable computation methods have been discovered for specific Ω if the policy is a specific parametric model (e.g., exponential families), thanks to the aforementioned studies. In Section 6, the underlying concept in Eq. (14) is that the bidirectional transformation between π_ϕ and ψ_ϕ implicitly occurs via its shared network parameters ϕ without extra computation costs. For example, in our implementation, both π_ϕ and ψ_ϕ are analytically drawn in closed-form expressions using the shared parameter ϕ by the following methods, respectively.

Discrete policies. Let the agent policy for a state $s \in \mathcal{S}$ be defined as $\pi_\phi(a|s) = p(a)$ for a discrete probability distribution on the action space, typically parameterized by a softmax distribution. Since the cardinality of action space is finite in this case, we can directly compute each output according to Definition 1, i.e., $\psi_\phi(s, a) = \Omega(p) + \nabla_p \Omega(p) - \sum_{a \in \mathcal{A}}$.

Continuous policies with the Shannon regularizer. For both discrete and continuous policies, the following equation holds: $\psi_\phi(s, a) = \log \pi_\phi(a|s)$ (pp. 4, Jeon et al. [18]). For multivariate Gaussians, we can analytically compute the log-likelihood. As stated in Appendix B.4, we applied the LDL decomposition on the covariance matrix Σ , which is a variant of Cholesky decomposition that ensures invertibility and positive-definiteness of the covariance matrix. In our experiments, this particular parameterization usually had significantly low numerical errors, thanks to the TensorFlow linear algebra libraries specialized for variants of the LU decomposition. See the work done by Pourahmadi [54] for more details for the parameterization.

Continuous policy with the Tsallis regularizer. Computing the operator Ψ_Ω for an arbitrary continuous policy is usually intractable when Ω is a Tsallis entropic regularizer except when the policy is constrained to be specific parametric models. In this work, we assumed the Gaussian policy, and the analytic form of $\Psi_\Omega(\Pi)$ was initially discovered by Nielsen and Nock [53]. The entire portion of Appendix B is dedicated to derivations of ψ_ϕ when Ω is a Tsallis entropic regularizer.

C.3 Network architectures

For all networks, we used 2-layer MLP with 100 hidden units. We considered the reward model with two separate neural networks (ψ_ϕ, d_ξ) for the proposed reward function for $\lambda \in \mathbb{R}^+$:

$$r_\phi(s, a) = \psi_\phi^\lambda(s, a) = \lambda \psi_\phi(s, a) + d_\xi(s),$$

Motivated by RAIRL-DBM, we considered the reward models in Fig. 10. The model outputs reward for proximal updates trained by mirror descent and state-only discriminator network. Discriminating state visitation by $d_\xi(\cdot)$ is required because the reward function needs to consider every state (especially the state that cannot be visited by π_E) until $D_{KL}(\rho_\pi \parallel \rho_{\pi_E}) \approx 0$. Fig. 10 (a) shows logits of the softmax distribution involved when calculating rewards when the action space is discrete. For continuous control (Fig. 10 (b)), the architecture is similar, where the mean and covariance are used to compute a reward for a particular action.

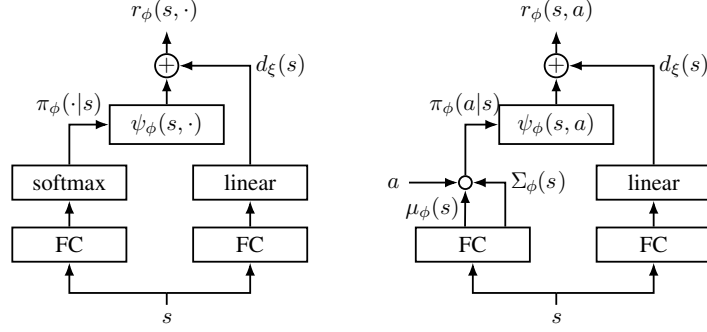


Figure 10: Schematic illustrations of MD-AIRL reward architectures for discrete (left) and continuous control (right)

C.4 Details on imitation learning data

The multigoal environment. Let the 2D coordinate denote the position of a point mass on the environment. In the multigoal environment, the agent, the point mass, is initially located according to the normal distribution $\mathcal{N}(\mathbf{0}, (0.1)^2 \mathbf{I})$. The four goals are located at $(6, 0)$, $(-6, 0)$, $(0, 6)$, and $(0, -6)$, where the agent can move a maximum of 1 unit per time step for each coordinate. The ground-truth reward is given by the difference between successive values of a Gaussian mixture depicted as the contour plot in Fig. 11.

Collecting expert demonstrations. For the multigoal environment and as well as MuJoCo benchmarks, we trained an expert policy using the SAC algorithm [55] and the demonstration data of IRL were collected from executing the trained RL expert. Only for the multigoal environment, the trajectories are post-processed to precisely capture optimal behavior (reaching each goal evenly). That is, we set the ratio of trajectories reaching each goal to exactly 25%.

C.5 Modeling policy with full covariance Gaussian distributions

We used the full covariance Gaussian distribution in this experiment (as well as the toy experiment in Fig. 2). Note that the covariance matrix is positive-definite and symmetric. To achieve numerically stable computation, we applied LDL decomposition in Appendix B.4 to model covariance matrix using unit lower- and upper-triangle matrices, and a diagonal matrix. As a result, the policy network outputs a vector $[\mu(s); \sigma(s); \mathbf{l}(s)]^\top$ for $s \in \mathcal{S}$ where the additional vector $\mathbf{l}(s)$ denotes $\frac{d(d-1)}{2}$ entries of unit lower triangular matrix. Denote $\mathbf{L}(s)$ as a unit lower triangular matrix from $\mathbf{l}(s)$. For example, the covariance matrix can be reconstructed by

$$\Sigma(s) = \mathbf{L}(s)[\text{diag}(\sigma(s))]\mathbf{L}(s)^\top.$$

In this case, the action samples can be efficiently calculated by

$$a = \mu(s) + \mathbf{L}(s)(\sigma(s) \cdot z) \quad z \sim \mathcal{N}(\mathbf{0}, \mathbf{I}) \quad (44)$$

Computing inverses, determinants and multiplications with unit triangular matrices and triangular and diagonal matrices can be efficiently performed by numerical libraries, where we used the accelerated linear algebra library from TensorFlow [56]. Therefore, we can efficiently model the Bregman divergence and reward using neural networks as provided in Appendix B. We clipped the standard deviation as $\sigma_i(s) \in [\ln 0.01, \ln 2]$ using \tanh for the stability. In MuJoCo experiments, instead of directly using squashed policies proposed in SAC [50], we assumed the application of \tanh as a part of the environment (known as *hyperbolized* environments of RAIRL [18]). Specifically, after an action a is sampled from the policies, we passed $\tanh(a/1.01) * 1.01$ to the environment. Then, we additionally clipped the hyperbolized actions to 1, if the given environment is not tolerant to the excessive values of action.

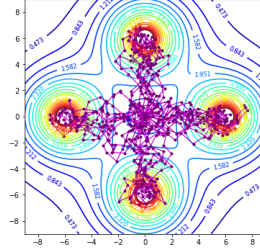


Figure 11: Visualization of the multigoal environment and expert trajectories.

C.6 Hyperparameters

Table 4: The bandit environments.

Parameter	Value
Learning rate (policy)	$1 \cdot 10^{-3}$
Learning rate (reward)	$1 \cdot 10^{-3}$
η_1	2.0
η_T	0.5
λ	1
Discount factor (γ)	0.0
Batch size	16
Steps per update	50
Total steps	300,000

Table 5: The multigoal environment.

Parameter	Value
Learning rate (policy)	$5 \cdot 10^{-4}$
Learning rate (reward)	$5 \cdot 10^{-4}$
Replay size	10,000
η_1	1.0
η_T	0.1
λ	1
Discount factor (γ)	0.5
Batch size	512
Steps per update	50
Total steps	300,000

Table 6: The MuJoCo environments.

Parameter	Hopper-v3	Walker2d-v3	HalfCheetah-v3	Ant-v3
Learning rate (policy)	$5 \cdot 10^{-4}$	$5 \cdot 10^{-4}$	$5 \cdot 10^{-4}$	$5 \cdot 10^{-4}$
Learning rate (reward)	$5 \cdot 10^{-4}$	$5 \cdot 10^{-4}$	$5 \cdot 10^{-4}$	$5 \cdot 10^{-4}$
Replay size	500,000	500,000	500,000	500,000
η_1	1.0	1.0	1.0	1.0
η_T	0.1	0.1	0.1	0.05
λ	0.01	0.01	0.01	0.001
Discount factor (γ)	0.99	0.99	0.99	0.99
Batch size	256	256	256	256
Steps per update	1,000	1,000	1,000	1,000
Initial exploration	10,000	10,000	10,000	10,000
Total steps	1,000,000	2,000,000	2,000,000	2,000,000

D Supplementary Experimental Results

Guessing the optimal choice of scheduling η_t for a short period of time is often challenging. Tab. 7 provides extended results of the experiments depicted in Fig. 2. The table contains the performance of imitation learning varies by series of $\{\eta\}_{t=1}^{100}$ controlled by two hyperparameters α_1 and α_T . These results substantially helped our hyperparameter choices of step sizes in the learning of MD-AIRL reward functions in Section 7.

Table 7: Bregman divergences $D_\Omega(\pi_t \parallel \pi_E)$ after the final steps ($T = 100$) with different step size scheduling (10 trials with different seeds).

(η_1, η_T)	Shannon ($q = 1$)	Tsallis ($q = 1.1$)	Tsallis ($q = 1.5$)	Tsallis ($q = 2$)
(2, 2)	-	1.19502 ± 0.64091	0.33996 ± 0.26144	0.68528 ± 0.46490
(1, 1)	0.08601 ± 0.07951	0.15432 ± 0.25206	0.22232 ± 0.31760	0.11193 ± 0.16801
(0.5, 0.5)	0.06707 ± 0.06042	0.07629 ± 0.06931	0.03801 ± 0.04611	0.06056 ± 0.05854
(0.2, 0.2)	0.01051 ± 0.00920	0.03221 ± 0.03239	1.21205 ± 0.00011	0.01805 ± 0.01587
(10, 1)	0.09861 ± 0.09546	-	1.09783 ± 0.53399	0.65887 ± 0.59846
(1, 0.1)	0.00706 ± 0.00863	0.00933 ± 0.01089	0.01660 ± 0.01152	0.02141 ± 0.00899
(1, 0.01)	0.01500 ± 0.01510	0.01109 ± 0.01405	0.02075 ± 0.02099	0.03348 ± 0.01901

The results indicate that scheduling η_t with a harmonic progression $\eta_1 = 1$ and $\eta_T = 0.1$ shows the overall best results in this experiment. From these results and our theoretical arguments, MD is recommended to gradually lower η_t , but the rate of change has to be carefully considered, especially when T is not significant. Thus, there are suitable scheduling ways of the step size η_t in practice, depending on Ω and T . As a rule of thumb, we recommend setting the initial step size close to 1 and scheduling to $\eta_T \approx 0$ when there is a reasonable amount of time for training.